FLOW INDUCED ACOUSTICS IN CORRUGATED PIPE

CHONG KOK YUNG

A project report submitted in partial fulfilment of the requirements for the award of Bachelor of Engineering (Hons.) Mechanical Engineering

Lee Kong Chian Faculty of Engineering and Science
Universiti Tunku Abdul Rahman

September 2015

DECLARATION

I hereby declare that this project report is based on my original work except for citations and quotations which have been duly acknowledged. I also declare that it has not been previously and concurrently submitted for any other degree or award at UTAR or other institutions.

Signature : _____

Name : Chong Kok Yung

ID No. : 11UEB06771

Date : 23 September 2015

APPROVAL FOR SUBMISSION

I certify that this project report entitled **"FLOW INDUCED ACOUSTICS IN CORRUGATED PIPE"** was prepared by **CHONG KOK YUNG** has met the required standard for submission in partial fulfilment of the requirements for the award of Bachelor of Engineering (Hons.) Mechanical Engineering at Universiti Tunku Abdul Rahman.

Approved by,

Signature : _____

Supervisor : Mr. King Yeong Jin

Date : 23 September 2015

Specially dedicated to

my beloved family members, lecturers and friends.

ACKNOWLEDGEMENTS

I would like to thank everyone who had contributed to the successful completion of this project. I would like to express my gratitude to my research supervisor, Mr. King Yeong Jin for his invaluable advice, guidance and his enormous patience throughout the development of the research. I am very fortunate to be blessed with the encouragement from him who had sacrificed his precious time to provide all the necessary information and assistance to me.

In addition, I would also like to express my gratitude to my loving parents and friends who had helped and given me encouragement along the process of completing this project.

Furthermore, I would also like to express my utmost gratitude to UTAR for providing me a golden opportunity to be involved in this research project as a partial fulfilment of the requirement for the degree of Bachelor of Engineering (Hons) Mechanical Engineering.

FLOW INDUCED ACOUSTICS IN CORRUGATED PIPE

ABSTRACT

Corrugated pipes are flexible pipes that are specially designed with corrugations to facilitate fluid flow between sea installations and surface equipment on drilling platforms. Nevertheless, corrugated pipes often experience self-sustained oscillations which leads to high intensity noise, known as "whistling" or "singing" during critical flow conditions. A special feature that can be observed in the flow of a corrugated pipe is known as shear layer which divides the high speed flow region from the low speed flow region next to the pipe wall. The formation of shear layer is normally noticed in a turbulent flow where the viscous sublayer adjacent to the wall does not have sufficient kinetic energy to travel against an adverse pressure gradient. Eventually, a separation of the boundary layer (shear layer) from the pipe wall is resulted at a cavity where there is abrupt pipe widening. The shear layers that are produced at the upstream of cavities are the source of sound due to its unsteadiness. In this study, the first aim is to investigate the flow pattern of the fluid passing through the corrugated pipe and the effect of pipe geometries on the whistling amplitude and peak whistling Strouhal number (Sr_{p-w}). Furthermore, optimal characteristic dimension is assessed and proposed. These aims are achieved through numerical simulation method by using a Computational Fluid Dynamics (CFD) software. The flow pattern of the fluid passing through the corrugated pipe and the effect of pipe geometries including cavity height (H), downstream edge radius (r_{down}), upstream edge radius (r_{up}), cavity width (W) and plateau (I) on the Sr_{p-w} and whistling amplitude are investigated using the proposed software. A ratio of $\frac{I}{W+r_{up}}$ is found to be a good indicator of the consistency of Sr_{p-w}. Furthermore, optimal characteristic dimension is also assessed among three different characteristic dimensions including $W + rup$, W and $\frac{I^2}{W+r_{up}}$. $\frac{I^2}{W+r_{up}}$ is found

to be the optimal characteristic dimension with smallest variation of Strouhal number. This finding is significant as it can allow us to avoid critical flow condition to minimize and prevent the whistling phenomenon more accurately and effectively by using the proposed equations. It is also possible to design the pipe parameters if the flow condition cannot be manipulated in certain conditions.

TABLE OF CONTENTS

LIST OF TABLES

LIST OF FIGURES

LIST OF SYMBOLS / ABBREVIATIONS

2D	two dimensional
c	speed of sound, m/s
dB	decibel
D_p	inner diameter of corrugated pipe, m
D_{sb}	diameter of side branch, m
f	frequency of oscillation, Hz
f_n	acoustic natural frequency of the pipe, Hz
H	depth of cavity or side branch, m
I	plateau, m
L_c	characteristic dimension, m
L_p	pipe length, m
L'	effective pipe length, m
n	mode number (1, 2, 3, ….)
Pt	pitch, m
r_{down}	downstream edge radius of cavity or side branch, m
r_{up}	upstream edge radius of cavity or side branch, m
Sr	Strouhal number
$Sr_{p\text{-}w}$	peak whistling Strouhal number
U	average flow velocity in the pipe, m/s
U_{cr}	critical flow velocity in the pipe, m/s
W	width of cavity of corrugated pipe, m
W_{eff}	effective cavity width of side branch, m
ρ_0	density of air, kg/m^3
$\lvert p' \rvert$	pressure wave's amplitude at a pressure anti-node, Pa
$\lvert u' \rvert$	acoustic velocity's amplitude at a pressure node, m/s

CFD	Computational Fluid Dynamics
FYP	Final Year Project
LES	Large Eddy Simulation

CHAPTER 1

INTRODUCTION

1.1 Background

Corrugated pipes are flexible pipes that are specially designed with corrugations to facilitate fluid flow between sea installations and surface equipment on drilling platforms. The main purpose of corrugations is to provide local stiffness and rigidity to prevent collapse of the pipe during bending while maintaining global flexibility. Nevertheless, corrugated pipes often experience self-sustained oscillations that leads to high intensity noise, known as “whistling” or “singing” during critical flow conditions.

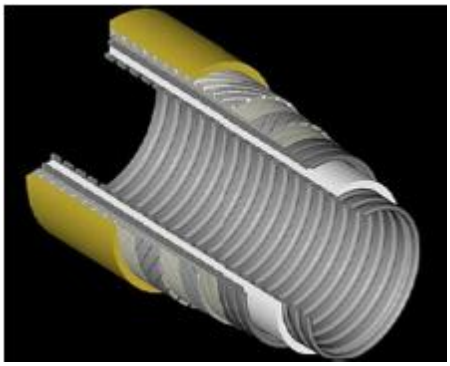

Figure 1.1: A Short Segment of a Typical Corrugated Pipe (Popescu et al., 2011)

A special feature that can be observed in the flow of a corrugated pipe as shown in Figure 1.1 (Popescu et al., 2011) is known as shear layer which divides the high

speed flow region from the low speed flow region next to the pipe wall. This is shown in Figure 1.2 (Popescu et al., 2011). The formation of shear layer is normally noticed in a turbulent flow where the viscous sublayer adjacent to the wall does not have sufficient kinetic energy to travel against an adverse pressure gradient. When this occurs, there will be a back flow along the pipe wall in the opposite direction to the main flow. Eventually, a separation of the boundary layer (shear layer) from the pipe wall is resulted at a cavity where there is abrupt pipe widening.

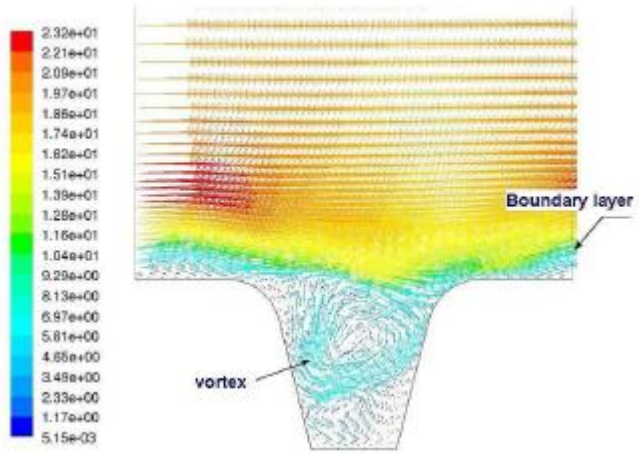

Figure 1.2: Shear Layer and Vortex in the Corrugation (Popescu et al., 2011)

According to Nakiboğlu et al. (2011), self-sustained oscillations is caused by interaction of shear layer instability with longitudinal local acoustic standing waves as defined in a feedback loop as shown in Figure 1.3 (Popescu et al., 2011). The shear layers that are produced at the upstream of cavities are the source of sound due to its unsteadiness. The acoustic sound waves in turn impose acoustic pressure which then triggers the rolling up of the shear layer into vortices. These vortices detach periodically to form vortex shedding. According to Popescu et al. (2011), a lock-in phenomena will occur where there is a resonance between longitudinal standing acoustic waves and vortex shedding when the frequency of vortex shedding coincides with the acoustic natural frequency of the pipe. The minimum fluid velocity for a lock-in to occur is known as onset velocity. Note that lock-in is a condition for whistling to occur but not every lock-in will result in whistling. In an investigation performed by

Nakiboğlu et al. (2010), whistling is not be noticed during the 1st acoustic mode. It is because the sources of sound are smaller than the viscous and radiation losses in the system. The first whistling or singing mode is therefore the 2nd acoustic mode but it varies from case to case basis.

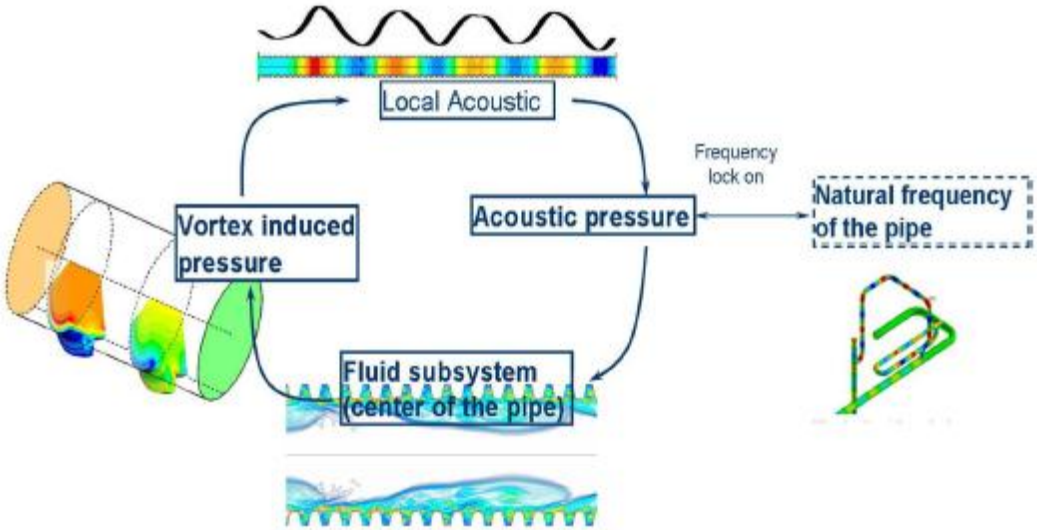

Figure 1.3: Feedback Loop between Hydrodynamic Subsystem and Acoustic Subsystem (Popescu et al., 2011)

Popescu et al. (2011) explained that the maximum shear layer instability is noticed in peak acoustic pressure variation regions. This finding shown that there is a strong coupling between fluid subsystem and acoustic subsystem. In overall, the shear layer unsteadiness (fluid flow subsystem) is affected and manipulated by the acoustic pressure that acts as a band pass filter to control synchronisation in the feedback loop. Besides, the longitudinal acoustic standing wave, which is the acoustic subsystem receives energy from the vortex-induced pressure variation that acts as an amplifier.

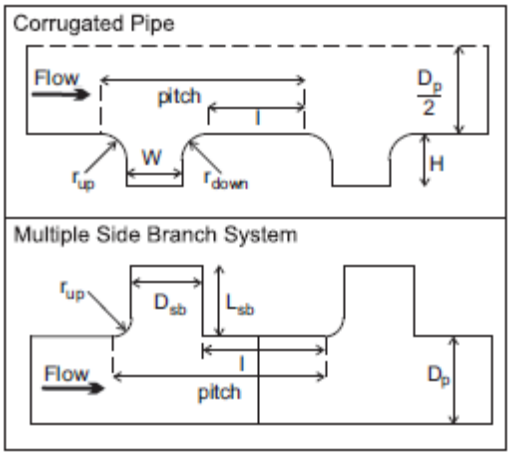

Figure 1.4: Geometric Charateristics of Corrugated Pipe and Multiple Side Branch System (Nakiboğlu et al., 2010)

Figure 1.4 (Nakiboğlu et al., 2010) shows the geometric characteristics of a corrugated pipe and a multiple side branch system. It is found that the certain geometric characteristics of a corrugated pipe can have significant effect to the flow and therefore the whistling phenomenon. However, investigation of the effects of all possible variations of geometric characteristics with corrugated pipe is very expensive and time consuming. Therefore, another similar periodic system, which is the multiple side branch system is often considered. It is important to note that although the side branches are non-axisymmetric, it does exhibit similar whistling characteristics as corrugated pipe (Nakiboğlu et al., 2011).

As shown in Figure 1.4 (Nakiboğlu et al., 2010), the pipe's inner diameter (D_p) is changing along the pipe length (L_p) in both systems periodically. In corrugated pipe, each cavity is in slit shape. Its width and depth are denoted as W and H respectively. On the other hand, the variation of pipe diameter in multiple side branch system is due to side branches along the core pipe, with diameter (D_{sb}) and depth (H). The radius of side branches and cavities are named as r_{up} and r_{down} for upstream and downstream edges, respectively. Besides, the wave length of the variation of pipe diameter is known as pitch (Pt). Last but not least, the plateau (I) is referring to the part with fixed diameter between two consecutive cavities or side branches.

1.2 Aims and Objectives

Basically, there are two main aims which are to be achieved in this project:

1. To analyse the flow pattern of the fluid passing through the corrugated pipe and the effect of pipe geometries on the peak whistling Strouhal number (Sr_{p-w}) and the whistling amplitude.

2. To assess and propose optimal characteristic dimension in calculating Strouhal number.

In order to achieve the aims stated, several objectives are defined:

1. To predict and estimate whistling amplitude and peak whistling Strouhal number (Sr_{p-w}) at different cavity height (H), downstream edge radius (r_{down}), upstream edge radius (r_{up}), cavity width (W) and plateau (I) by using CFD simulation software.

2. To construct and analyse tables and graphs from sets of whistling amplitude and Sr_{p-w} from the CFD simulation software.

3. To compare and choose optimal characteristic dimension through collection of Sr_{p-w} from 11.61m/s to 21.61m/s with 3 types of characteristic dimension using CFD simulation software.

In this study, numerical method is used to determine the Sr_{p-w} and the whistling amplitude. The numerical simulations are performed by using a Computational Fluid Dynamics (CFD) simulation software. The results obtained from numerical simulations are studied to investigate the phenomenon of flow induced acoustics in the corrugated pipe.

This research project consists of a number of limitations:

1. In reality, the corrugated pipe is interacted with moving sea water externally as shown in Figure 1.5 (Gao et al., 2011). This imposes a vortex induced vibration on the corrugated pipe. According to Nakiboğlu et al. (2010), the spatial coherence will be enhanced and a stronger whistling sound will be produced with a frequency that is compromise between the mechanical resonance frequency and the vortex shedding frequency if a mechanical vibration is induced. However, the effect of flow induced vibration on the whistling phenomenon is neglected in this project.

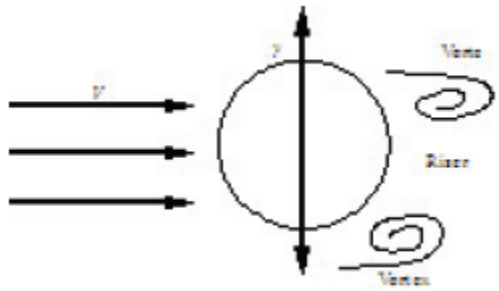

Figure 1.5: External Flow Across the Riser (Gao et al., 2011)

2. In addition, the possible damping effect of the water external to the corrugated pipe is also assumed to be negligible. The project is mainly focused on the effect of geometric parameters and the flow across the corrugations to the whistling phenomenon.

In this report, the findings related to the topic of the project will be first discussed and commented in Chapter 2. In Chapter 3, the details of the numerical simulation method are explained. In the subsequent chapter (Chapter 4), the results collected are presented, analysed and discussed. This is followed by the last chapter (Chapter 5) in which the conclusions are drawn and recommendations for further research are made.

CHAPTER 2

LITERATURE REVIEW

2.1 Strouhal Number and Whistling Amplitude

Two terminologies that are closely related to the flow induced acoustics in corrugated pipe are known as Strouhal number and whistling amplitude. These two terms are explained in the following sub-sections.

2.1.1 Strouhal Number

An important dimensionless parameter that is normally used to characterise the oscillating flow is known as Strouhal number (Sr).

$$Sr = \frac{fL_c}{U} \tag{2.1}$$

where

f = oscillation frequency, Hz

L_c = characteristic dimension, m

U = average flow velocity in the pipe, m/s

According to Nakiboğlu et al. (2011), as the average flow velocity increases, the frequency of whistling shows only slight increase in a particular resonant mode. As a result, the Strouhal number actually decreases at each mode and hence a range of Strouhal numbers will be noticed. The greatest value of Strouhal number in a specific

mode is known as critical Strouhal number (Sr_{cr}). After that, the rise of average flow velocity increases the sound amplitude until it reaches a maximum value. The Strouhal number at peak sound amplitude at a particular acoustic mode is known as peak whistling Strouhal number (Sr_{p-w}). Nakiboğlu et al. (2010) explained that Sr_{p-w} is obtained through a plotting of global gradient of consecutive modes.

Nakiboğlu et al. (2010) claimed that the sum of the width of cavity and the upstream edge radius, $W + r_{up}$, which is also known as modified gap width is the best representation of characteristic dimension. In the study of Nakiboğlu et al. (2010) with 14 different configurations corrugated pipes, the optimum characteristic dimension was determined among pitch ($Pt = r_{up} + W + r_{down} + l$), gap width ($r_{up} + W + r_{down}$) and modified gap width ($W + r_{up}$). It is observed that the use of the foregoing characteristic dimension resulted in $0.45 \leq Sr \leq 0.8$, $0.30 \leq Sr \leq 0.42$ and $0.32 \leq Sr \leq 0.42$, respectively. Modified gap width is therefore the optimum characteristic dimension as the range of Strouhal number is smaller.

2.1.2 Whistling Amplitude

Another important parameter that is commonly used to specify the maximum whistling amplitude is known as dimensionless sound amplitude, which is defined as (Nakiboğlu and Hirschberg, 2012):

$$\frac{|p'|}{\rho_0 c U} = \frac{|u'|}{U} \tag{2.2}$$

where

$|p'|$ = pressure wave's amplitude at a pressure anti-node, Pa

ρ_0 = density of air, kg/m^3

c = speed of sound, m/s

U = velocity of main flow, m/s

$|u'|$ = acoustic velocity's amplitude at a pressure node, m/s

2.2 Similarities and Differences between Corrugated Pipe and Multiple Side Branch System

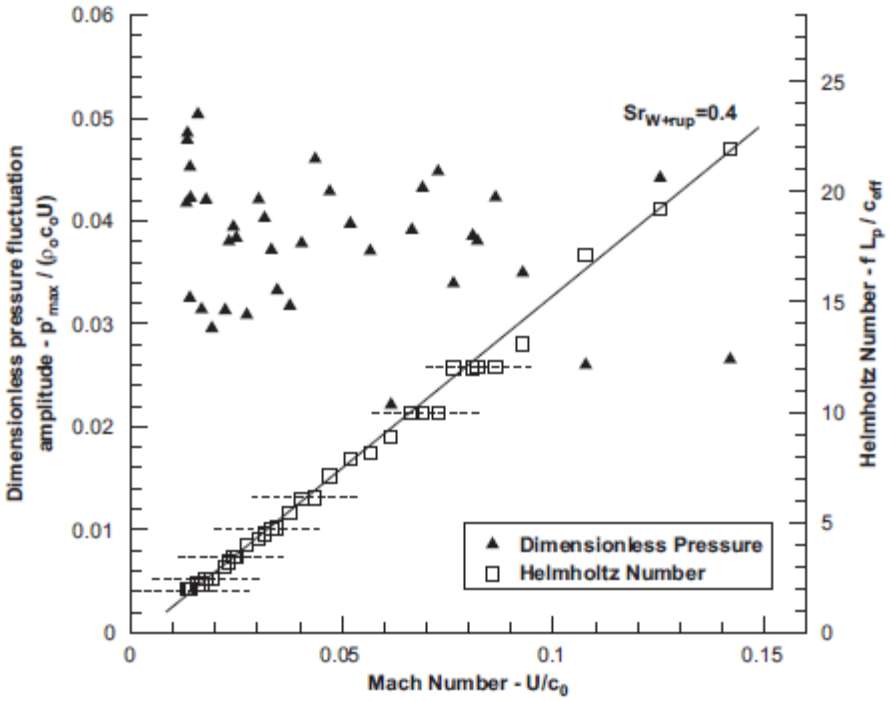

Figure 2.1: Helmholtz Number and Dimensionless Sound Amplitude v. Mach Number for a Typical Corrugated Pipe (Nakiboğlu et al., 2010)

Nakiboğlu et al. (2010) had performed experiment on both corrugated pipes and multiple side branch system to study their whistling behaviour. As shown in Figure 2.1 (Nakiboğlu et al., 2010), the average increase of frequency is approximately linear. However, some plateaus can be revealed where the frequencies are not rising continuously with rising velocity. These plateaus are actually corresponding to the lock-in at each longitudinal pipe mode. Besides, it is also observed that pressure amplitude changes non-monotonically with velocity. There is a local maximum at each lock-in.

There are also many similarities between corrugated pipe and multiple side branch system. One of the similarities is that the frequency (Helmholtz number) is a non-decreasing piecewise constant function of Mach number as mentioned earlier. As seen in Figure 2.2 (Nakiboğlu et al., 2010), Helmholtz number of 1, 1.5, 2, 2.5… corresponds to 2nd, 3rd, 4th, 5th… lock-in of the multiple side branch system, respectively. Besides, a global constant slope can also be observed between Helmholtz number and Mach number, which is the Sr_{p-w} for the pipe. These characteristics are also observed in corrugated pipe.

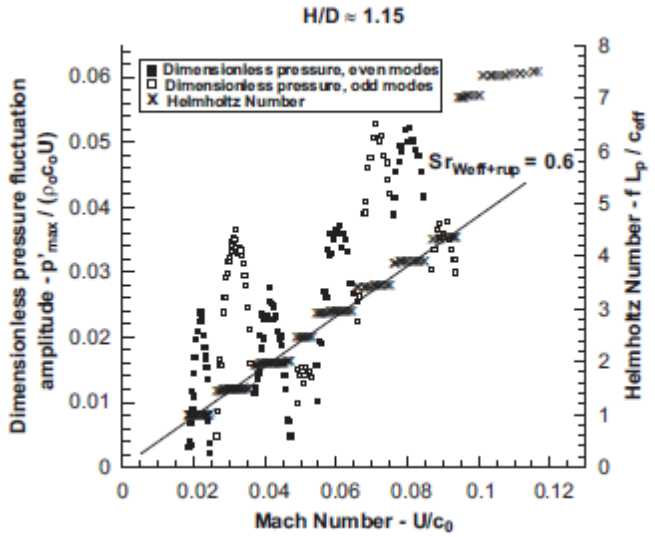

Figure 2.2: Helmholtz Number and Dimensionless Sound Amplitude v. Mach Number for a Multiple Side Branch System (Nakiboğlu et al., 2010)

In addition, Nakiboğlu et al. (2010) also explained that singing or whistling could not be noticed for the 1st mode in both types of system. It is because the sources of sound are smaller than the viscous and radiation losses in the system. The first whistling or singing mode is therefore the 2nd acoustic mode for corrugated pipe and multiple side branch system.

On the other hand, it is determined from the experiment that the Sr_{p-w} are different for both geometrically periodic systems. From the experiment conducted by Nakiboğlu et al. (2010), the Sr_{p-w} are $0.32 \leq Sr_{W+r_{up}} \leq 0.5$ and $0.5 \leq$

$Sr_{W_{eff}+r_{up}} \leq 0.6$ for corrugated pipe and multiple side branch system, respectively. In a study conducted by Nakiboğlu et al. (2011), it was found that this result is caused by different velocity profile found in both systems due to different proportion of pipe diameter to the sum of width of cavity and upstream edge radius (confinement ratio).

One of the main differences between both systems is that corrugated pipe has slit shaped cavities whereas the side branches of multiple side branch system are circular in cross sections. According to Nakiboğlu et al. (2010), the side branch diameters can be represented in effective cavity width as:

$$W_{eff} = \frac{\pi D_{sb}}{4} \tag{2.3}$$

where

D_{sb} = diameter of side branch, m

Hence, for multiple side branch system, the total of effective cavity width and upstream edge radius ($W_{eff} + r_{up}$) is used as the characteristic dimension.

In addition, the corrugated pipes used in the experiment have 2 x 10^2 corrugations but the multiple side branch system has only 19 side branches. It is normally found that corrugated pipes have higher whistling frequencies compare to multiple side branch system. However, the corrugation quantity per wave length in corrugated pipe at high frequencies (Helmholtz number) is closed to that of multiple side branch system at low frequencies. Therefore, the lowest modes in the multiple side branch system are of main concern.

2.3 Effect of Different Pipe Geometries

In this sub-section, the consequences of different pipe geometries to Sr_{p-w} and whistling amplitudes are reviewed.

2.3.1 Effect of Pipe Termination

Nakiboğlu et al. (2010) had studied the effect of pipe termination on the whistling amplitude. Two different types of pipe termination which are sharp termination and whistler type nozzle termination were used in the experiment as shown in Figure 2.3 (Nakiboğlu et al., 2010). It is found that sharp termination gave a stronger sound absorption compare to whistler type nozzle termination.

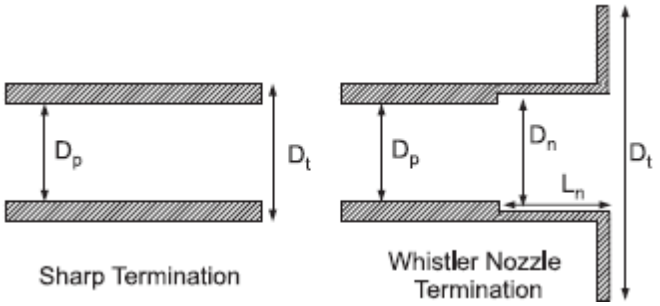

Figure 2.3: Sharp and Whistler Nozzle Terminations (Nakiboğlu et al., 2010)

2.3.2 Effect of Edge Shape

Nakiboğlu et al. (2010) discovered that rounding of upstream edge radius of cavity (r_{up}) is able to reduce the initial sound absorption and increase the whistling amplitude by a factor of 3 to 5. However, the rounding of downstream edge radius of cavity (r_{down}) produced a minor effect on the whistling amplitude. This is because the shear layer thickness becomes less concentrated as the downstream edge is approached.

2.3.3 Effect of Cavity Depth

According to Nakiboğlu et al. (2010), the Sr_{p-w} and the dimensionless sound amplitude are almost constant for a deep cavity ($0.61 \leq H/D_{sb} \leq 1.15$). In the range of $0.18 \leq H/D_{sb} \leq 0.55$ (shallow cavity), it is observed that the Sr_{p-w} and the

dimensionless sound amplitude are increasing with increasing H/D_{sb} ratio. Besides, the dimensionless sound amplitudes are found to be low (less than 3×10^{-3}) in the range of $0.25 \leq H/D_{sb} \leq 0.50$.

2.3.4 Effect of Pitch Length

Nakiboğlu et al. (2011) claimed that the Sr_{p-w} is not a function of pitch. However, Popescu et al. (2011) argued that the pitch length does influence the Strouhal number. It is shown in the simulation results tabulated by Popescu et al. (2011) that the Strouhal number is much lower for the cavity with longer pitch length. Popescu et al. (2011) further explained that this is because the longer the pitch, the longer the period of interaction between vortices.

2.3.5 Effect of Confinement Ratio

Confinement ratio is the ratio of pipe diameter to cavity width (D_p/W). In most of the cases, the upstream cavity edge is rounded. Therefore, confinement ratio is normally the proportion of pipe diameter to the sum of width of cavity and upstream edge radius $\left[D_p/(W + r_{up})\right]$. From the experiment by Nakiboğlu et al. (2011), it is observed that the Sr_{p-w} decreases as the confinement ratio increases. This is also confirmed with the numerical method proposed by Nakiboğlu et al. (2011). According to Nakiboğlu et al. (2011), the alteration in Sr_{p-w} is caused by the variation in the flow profile when there is an change of confinement ratio.

2.3.6 Effect of Pipe Length

Nakiboğlu et al. (2011) had found that the variation of pipe length does not affect the Sr_{p-w} from the experiment. Besides, there is an increase of dimensionless sound amplitude with increasing commercial corrugated pipe length until L/D_p of 100 with $|u'|/U \approx 0.1$, beyond which there is no change of dimensionless sound amplitude. A similar phenomenon was also observed in PVC corrugated pipe which saturated at L/D_p of 60 with $|u'|/U \approx 0.1$. Besides, the saturation in dimensionless sound amplitude was observed in multiple side branch system with 19 side branches at $|u'|/U \approx 0.35$.

2.3.7 Effect of Plateau Length

Nakiboğlu and Hirschberg (2012) mentioned that the peak whistling amplitude and the Sr_{p-w} are both affected by the hydrodynamic interference between cavities.

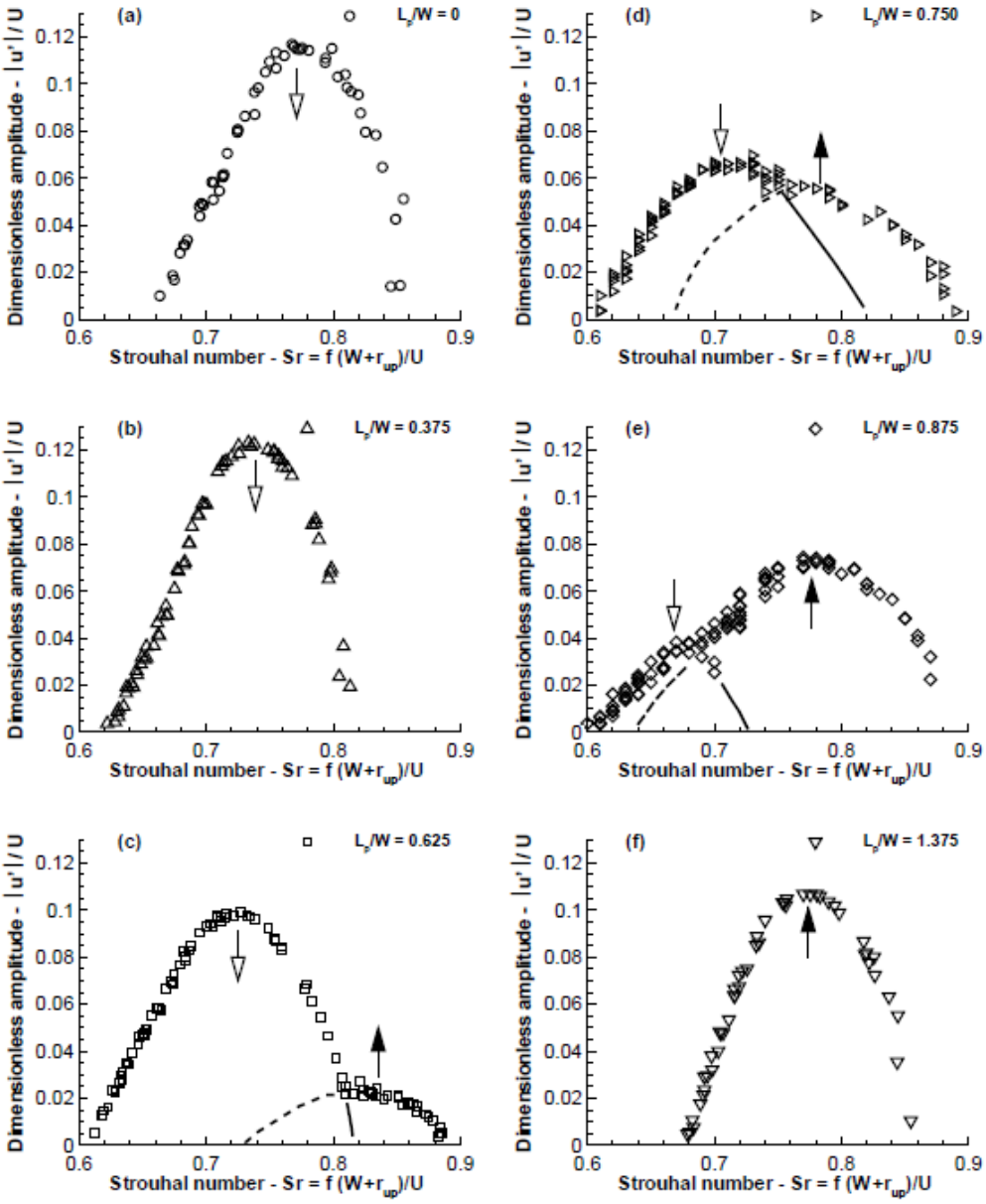

Figure 2.4: Dimensionless Fluctuation Amplitude Plotted v. Strouhal Number for Plateau Length to Cavity Width Ratios of L_p/W = 0, 0.375, 0.625, 0.750, 0.875 and 1.375 (Nakiboğlu and Hirschberg, 2012)

As shown in Figure 2.4 (Nakiboğlu and Hirschberg, 2012), there is a single peak (primary peak) when plateau length to cavity width ratio, L_p/W= 0. As L_p/W increases, there is a decrease in fluctuation amplitude and the peak also shifts to lower Strouhal number. A secondary peak can then be observed when the L_p/W is increased to 0.625. As L_p/W is further increased, the secondary peak increases in fluctuation

amplitude and it also shifts to lower Strouhal number. Eventually, the secondary peak replaces the primary peak at the same Strouhal number and similar pressure amplitude as that of L_p/W=0 when L_p/W reaches 1.375.

2.3.8 Source Localisation

Nakiboğlu et al. (2010) had found that noise is mainly produced in the pressure nodes of the longitudinal standing waves along the pipe where the grazing acoustic velocity is maximum. The magnitude of sound dropped significantly with plugs at the pressure node.

2.4 Effect of Different Velocity Profiles

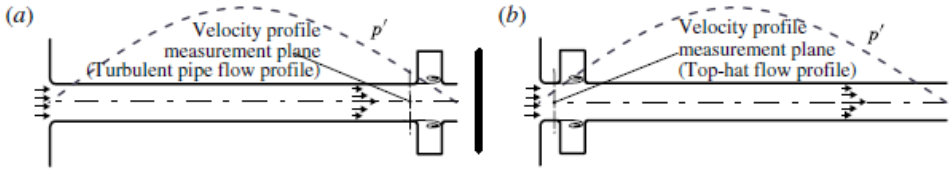

Figure 2.5: Two Different Corrugated Pipe Configurations Investigated (Nakiboğlu et al., 2012)

The test was conducted on 2 types of corrugated pipe configuration, with cavity close to the downstream (Configuration A) and cavity close to the upstream (Configuration B) as shown in Figure 2.5 (Nakiboğlu et al., 2012). According to Nakiboğlu et al. (2012), the cavity in configuration B was subjected to top-hat velocity profile with a thin boundary layer whereas the cavity in configurations A was subjected to turbulent approach velocity profile.

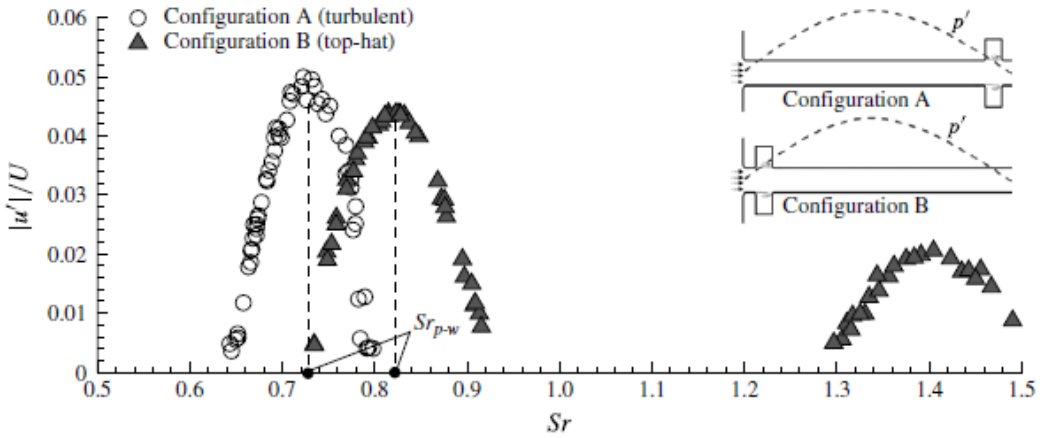

Figure 2.6 : Dimensionless Sound Amplitude v. Strouhal Number for Configurations A and B (Nakiboğlu et al., 2012)

Firstly, there is only single range of Strouhal numbers whereby the singing or whistling is noticed for Configuration A as shown in Figure 2.6 (Nakiboğlu et al., 2012). However, there are two different ranges of Strouhal numbers whereby the whistling phenomenon is observed in Configuration B. Nakiboğlu et al. (2012) stated that this is because configuration A has weaker hydrodynamic amplification at higher Strouhal number range due to its thicker initial shear layer momentum thickness. Secondly, it is also observed that Configuration B has higher Sr_{p-w} than Configuration A in the lower range of whistling Strouhal numbers. According to Nakiboğlu et al. (2012), this is due to the difference in the shear layer momentum thickness for two different configurations.

2.5 Numerical Method Involving Incompressible Flow Simulations and Vortex Sound Theory

Nakiboğlu et al. (2011) had investigated both types of geometric similar system by using experimental method and numerical method which combines incompressible flow simulations and Vortex Sound Theory. The numerical method is able to capture

the non-linear saturation of shear layer and predict the effect of pipe geometric characteristics on Sr_{p-w} and dimensionless sound amplitude fairly well.

Nevertheless, the numerical method has some limitations. In the numerical method, the hydrodynamic interference between the cavities are assumed to be negligible. However, according to Nakiboğlu and Hirschberg (2012), the hydrodynamic interaction does affect both the Sr_{p-w} and dimensionless sound amplitude. This is also highlighted in sub-section 2.3.7. Besides, the numerical method introduced does not include turbulence modelling, which is important for shallow cavities ($H/W \leq 0.5$). Fortunately, most of the industrial applications corrugated pipes have deep cavities.

Furthermore, the use of Kirchhoff theory in approximation of acoustic damping coefficient might also lead to over prediction of sound amplitudes in long corrugated pipe. The method used to estimate visco-thermal losses should also be improved. Last but not least, a traveling wave model should be used for very long corrugated pipe instead of a standing wave model.

A similar numerical method is also applied in a study of aeroacoustics behaviour of flow inside T-joints by Martinez-Lera, Golliard and Schram (2010). The 3 steps involved in this method are incompressible CFD simulation, sound sources post processing based on vortex sound theory and transfer function identification. According to them, CFD simulations are very computational efficient as it is possible to obtain wide range of valuable information at a low computational cost. They have also verified that this method can produce results which are consistent with the experimental method. Therefore, this numerical method is very favourable for engineering applications.

For this project, a numerical method based on incompressible 2D CFD simulation is also proposed. This is further discussed in the following chapter.

CHAPTER 3

METHODOLOGY

3.1 Gantt Chart and Flow Chart

As shown in Figure 3.1 is the flow chart for conducting the entire final year project (FYP). Besides, the Gantt chart for conducting the entire FYP is also shown in Table 3.1 and Figure 3.2 with durations, start data, finish data and predecessors stated.

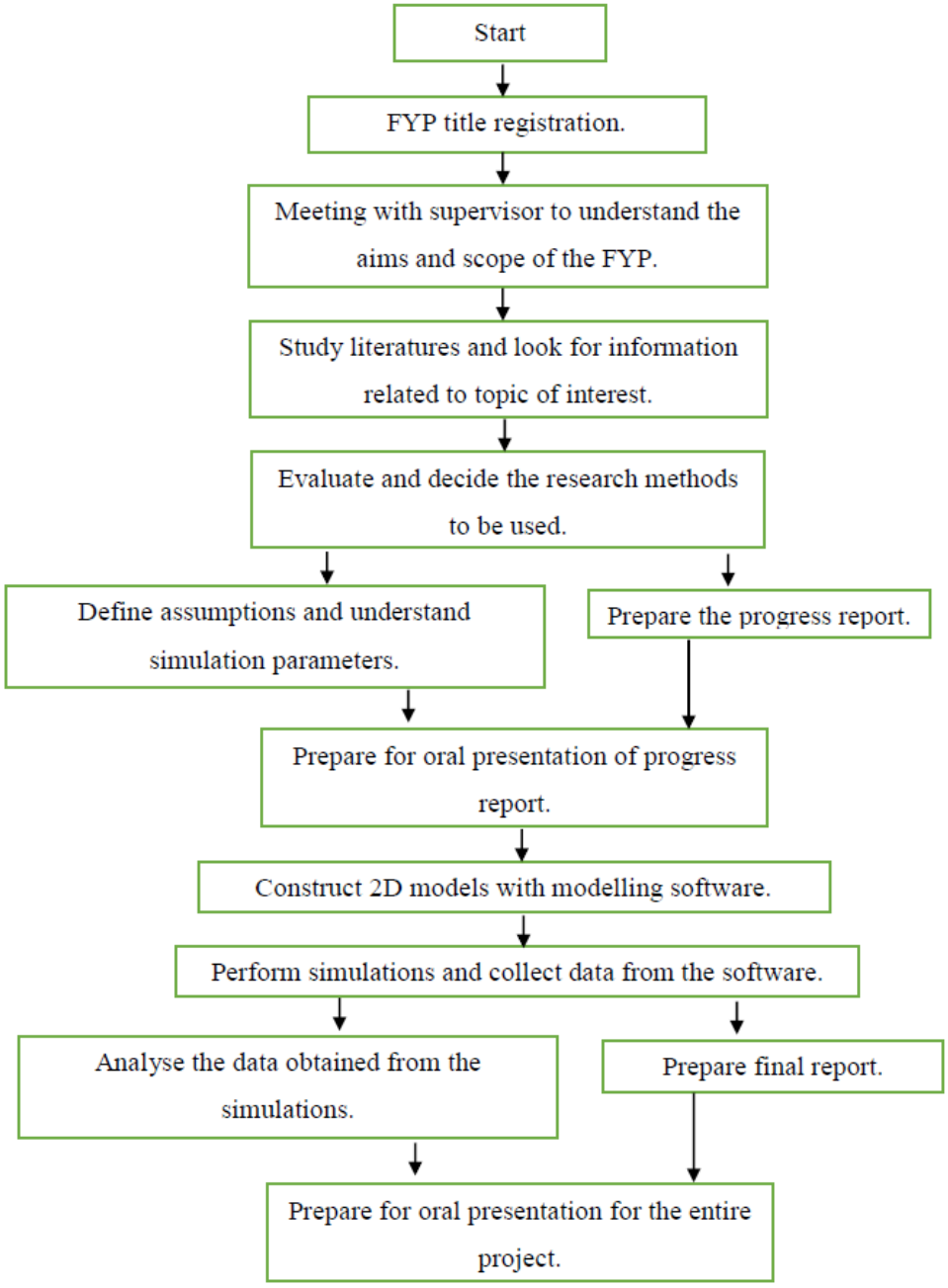

Figure 3.1: Flow Chart for FYP Progress

Table 3.1: Gantt Chart Table for FYP Progress

No.	Task	Start Date (DD/MM/YY)	Finish Date (DD/MM/YY)	Duration (Days)	Predecessors
1	FYP title registration.	14/01/2015	20/01/2015	7	-

2	Meeting with supervisor to understand the aims and scope of the FYP.	21/01/2015	21/01/2015	1	1
3	Study literatures and look for information related to topic of interest.	22/01/2015	10/02/2015	20	2
4	Evaluate and decide the research methods to be used.	11/02/2015	20/02/2015	10	3
5	Define assumptions, understand simulation parameters.	21/02/2015	17/03/2015	25	4
6	Prepare the progress report.	21/02/2015	11/04/2015	50	4
7	Prepare for oral presentation of progress report.	12/04/2015	18/04/2015	7	6
8	Construct 2D models with modelling software.	08/06/2015	27/06/2015	20	7
9	Perform simulations and collect data from the software.	28/06/2015	27/07/2015	30	8
10	Analyse the data obtained from the simulations.	28/07/2015	16/08/2015	20	9
11	Prepare final report.	28/07/2015	26/08/2015	30	9
12	Prepare for oral presentation for the entire project.	27/08/2015	13/09/2015	18	11

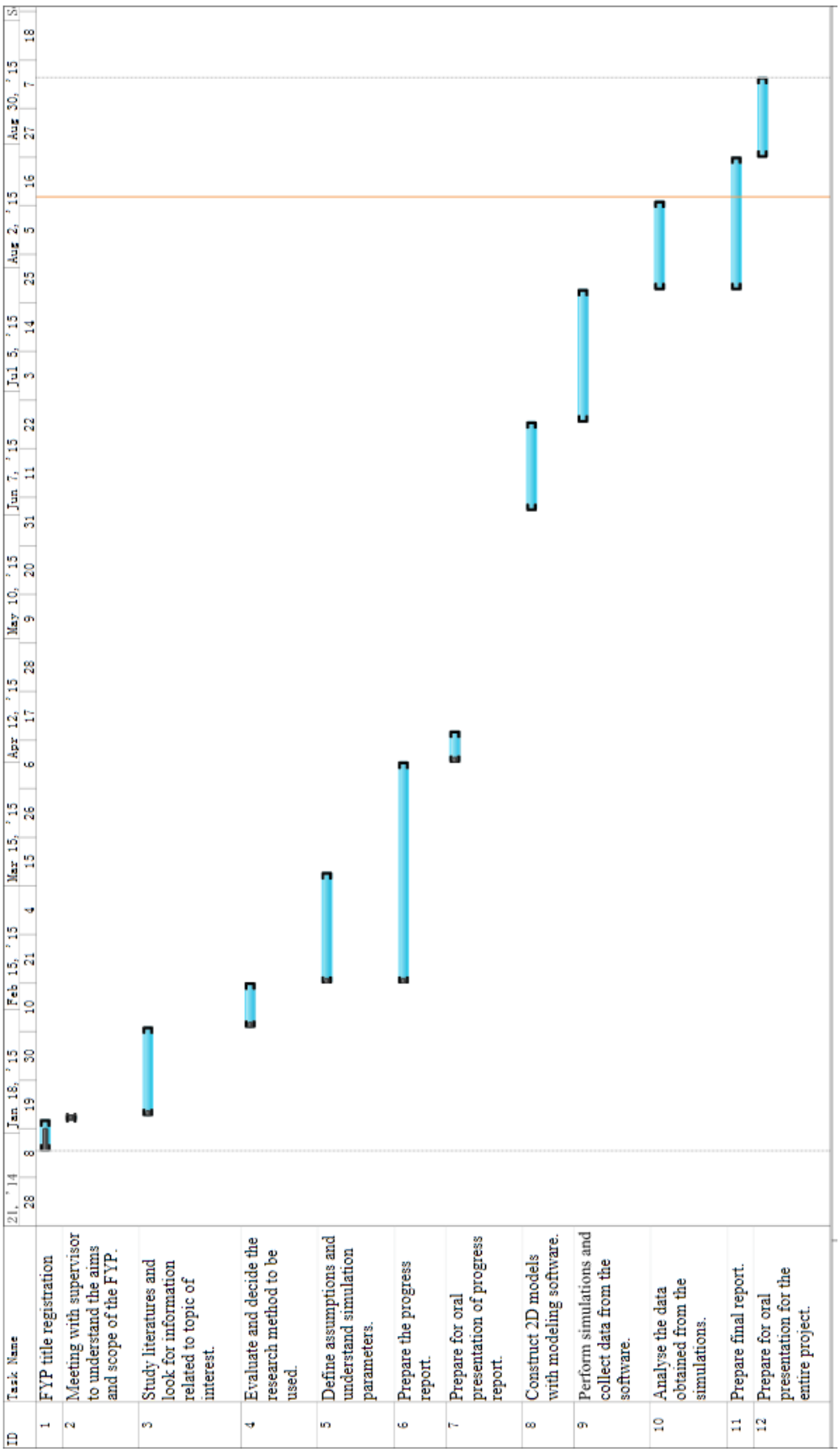

Figure 3.2: Gantt Chart for FYP Progress

3.2 Numerical Method

3.2.1 Assumptions

In addition to some limitations that are stated in Section 1.2, some assumptions are also made in the simulations. These assumptions are:

1. Representation of entire flow condition with only single cavity. This has two limitations, which are lack of a resonance condition and lack of lock-on mechanism. However, according to Popescu et al. (2011), flow across a single cavity does give sufficient information on the acoustic pressure wave sources' characteristics in the corrugated pipes.

2. Two dimensional flow. Since the corrugated pipe is uniform across its cross section, 2D model is suitable. This can also reduce the sketching time and computational time.

3. Flow in single direction. The flow in the corrugated pipe is assumed to flow uniformly in x direction (horizontal).

4. Replacement of rounded shape of cavity bottom with straight edges. Popescu et al. (2011) mentioned that the cavity bottom has not much influence on the flow field. It is therefore beneficial to straighten the cavity bottom so that the sketching process is easier and computational time is shorter.

5. Incompressible flow. For air flow at the range of 10m/s to 20m/s, this assumption is reasonable as it is below sonic level. With this assumption, the simulation is simplified and the computational time is shorten.

6. The outlet of the cavity is defined as pressure outlet whereas the inlet of the cavity is defined as velocity inlet.

3.2.2 Simulation Steps

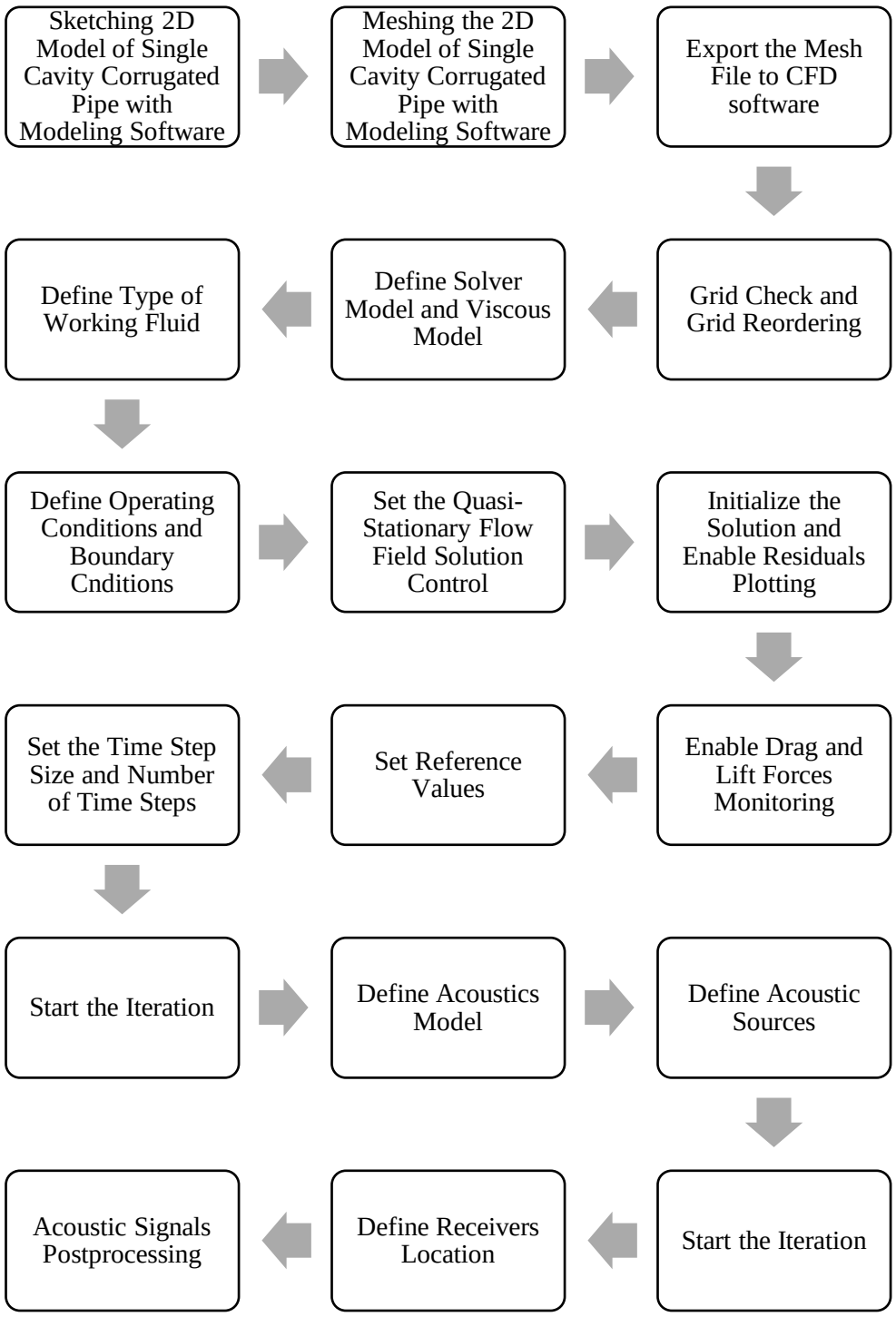

Figure 3.3: Flow Chart for Simulation Steps

As shown in Figure 3.3 are the important steps that are involved in the simulation work. First and foremost, it is necessary to sketch and mesh the 2D model of single cavity corrugated pipe. In this project, these two important procedures are performed by using a modelling software. As shown in Figure 3.4, quadrilateral cells are used instead of triangular cells because they generate less numerical diffusion in Large Eddy Simulation (LES). After the 2D model is saved, it is exported to the CFD software.

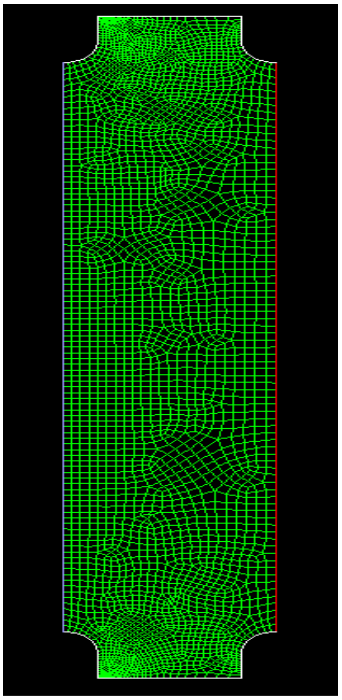

Figure 3.4: 2D Model of Single Cavity Corrugated Pipe

Once the mesh file is imported into CFD software, it is necessary to perform grid check and grid reordering. This process is important in reducing the bandwidth so that the subsequent solutions can be processed faster.

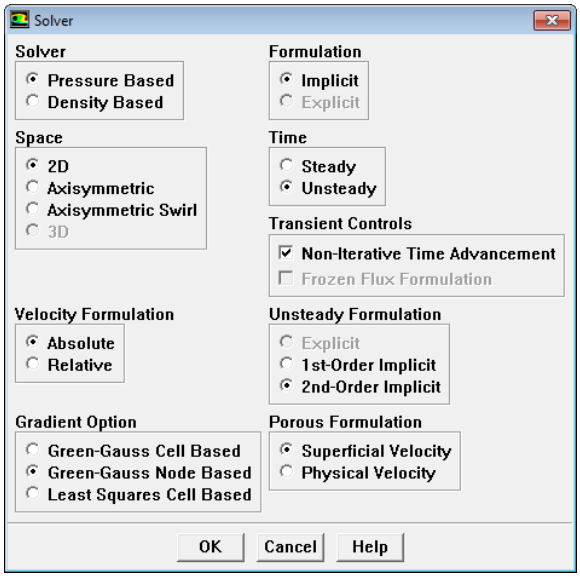

Figure 3.5: Solver Model Setting

The next step is to define the solver model and viscous model. In solver model, pressure based implicit solver with second order implicit unsteady formulation is used as shown in Figure 3.5. Besides, non-iterative time advancement is used in transient controls so that the simulation process is speeded up. On the other hand, Large Eddy Simulation (LES) turbulence model is used as the viscous model as shown in Figure 3.6. It is very suitable for aero-acoustic simulations because it resolves all eddies with scales larger than grid scale but eliminates small scales of the solution. This is good enough as large eddies possess most energy and interact more strongly with the flow. As a result, wide band aero-acoustic noise can be well predicted.

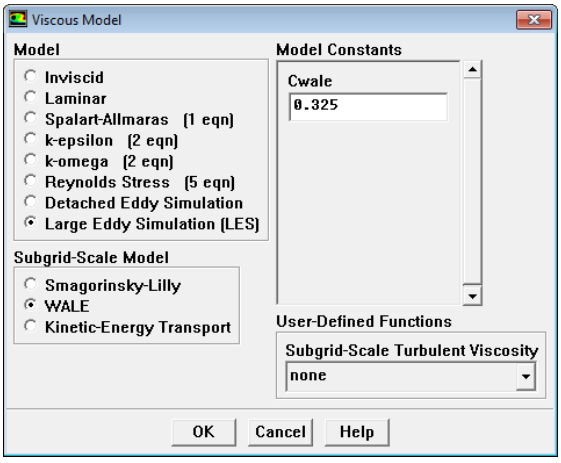

Figure 3.6: Viscous Model Setting

After that, it is important to define some input parameters such as type of working fluid (air), operating pressure (101325 Pa) and boundary conditions. The outlet of the cavity is defined as pressure outlet whereas the inlet of the cavity is defined as velocity inlet as shown in Figure 3.7.

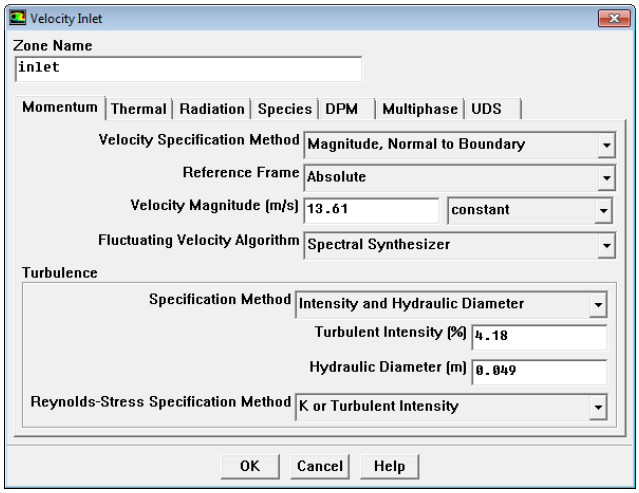

Figure 3.7: Inlet Boundary Condition

Before proceeding to acoustic analysis, it is necessary to establish quasi stationary flow field solution controls to ensure the drag and lift forces are oscillatory and periodic in nature. As shown in Figure 3.8, PISO is selected for pressure-velocity coupling whereas PRESTO! and second order upwind are chosen as pressure and momentum discretization methods, respectively. In fact, PRESTO! is a very accurate method for interpolating face pressure values from cell pressures.

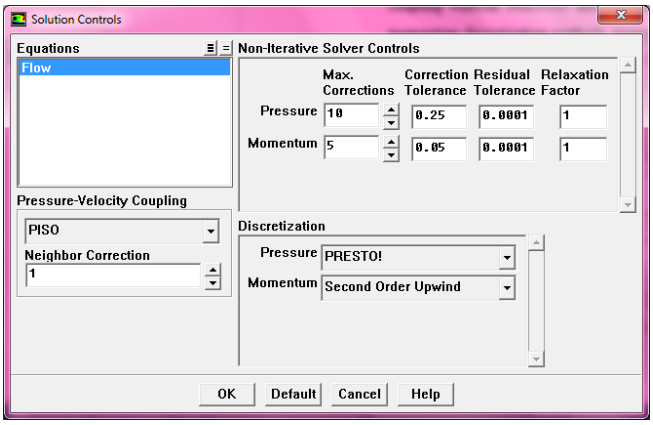

Figure 3.8: Quasi Stationary Flow Field Solution Controls

Then, the solution is initialised from the inlet and the drag and lift forces monitoring are enabled. It is also required to set the reference values as shown in Figure 3.9 which are necessary in calculation of drag coefficient, lift coefficient and Strouhal number.

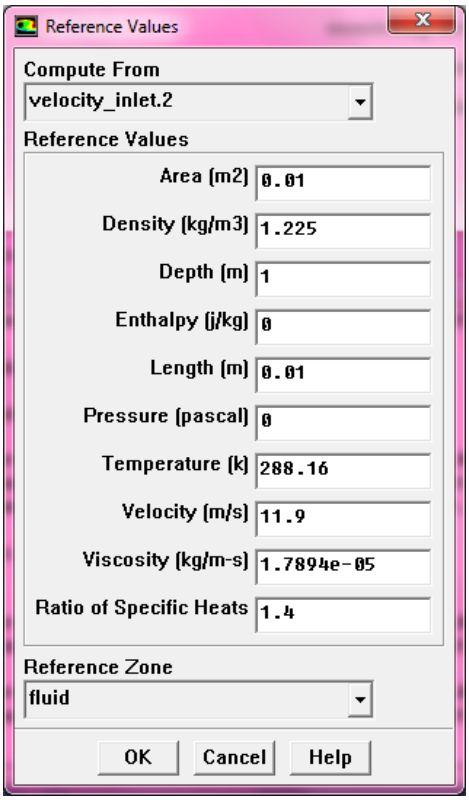

Figure 3.9: Reference Values

Thereafter, the time step size and number of time step are set. Note that the smaller the time step size, the more accurate is the simulation results. Hence, time step size of 1e-05 is used in this project. Besides, the number of time step is set to 5000 so that a stable solution will be achieved. In other words, the acoustic signals will be recorded for a duration of 0.05s.

Before defining the acoustic model, the iteration is started to ensure drag and lift forces are periodic and oscillatory in nature as shown in Figure 3.10 and Figure 3.11 respectively.

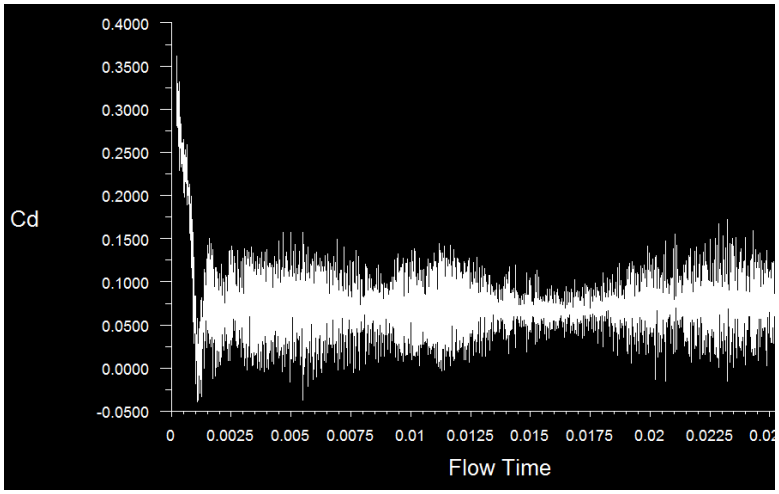

Figure 3.10: Coefficient of Drag

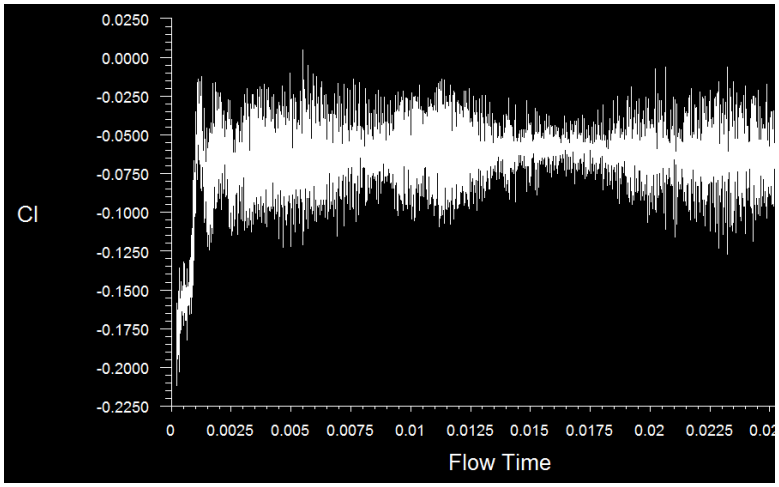

Figure 3.11: Coefficient of Lift

Subsequently, the acoustic model is set according to Figure 3.12. Ffows-Williams & Hawkings model is chosen while the other model constants are retained as default. Furthermore, the acoustic source is defined as shown in Figure 3.13 before the simulation is run again. Once the simulation is completed, it is necessary to reset the Source Correlation Length to the sum of pipe diameter and two cavities' depth. This is very important in 2D aero-acoustic calculations as the software will build a source volume internally with a depth equal to the value of Source Correlation Length and all sources outside this volume will be ignored. This will affect the sound pressure level obtained in the results.

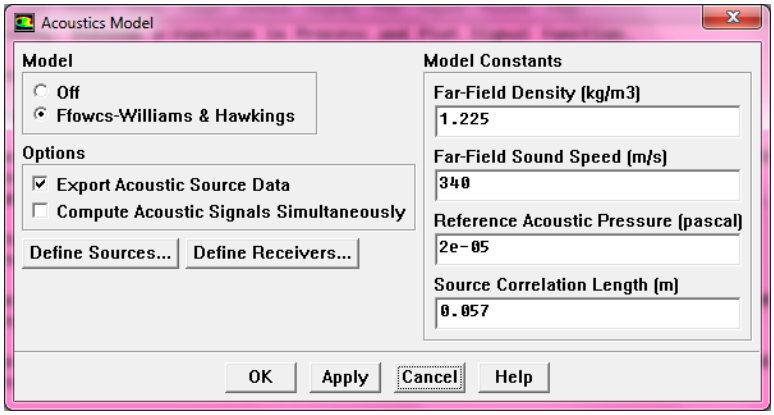

Figure 3.12: Acoustic Model Setting

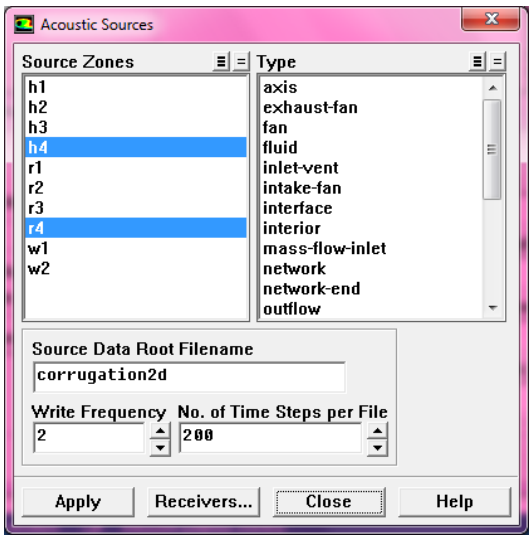

Figure 3.13: Acoustic Sources Setting

Last but not least, the positions of the acoustic receivers should be defined so that the sound level and frequency can be captured. In every case, two receivers are used. The locations these receivers are shown in Figure 3.14. For consistency purpose, the receiver 1 was located at 0.5mm from the wall in positive x direction while the receiver 2 was located at 0.5mm from the wall in negative x direction. Both receivers are located at the same level as pipe diameter in all cases. Figure 3.15 shows the positions of receivers in one of the geometries that was tested in the simulations. After that, the receivers are added to the File XY plot as shown in Figure 3.16.

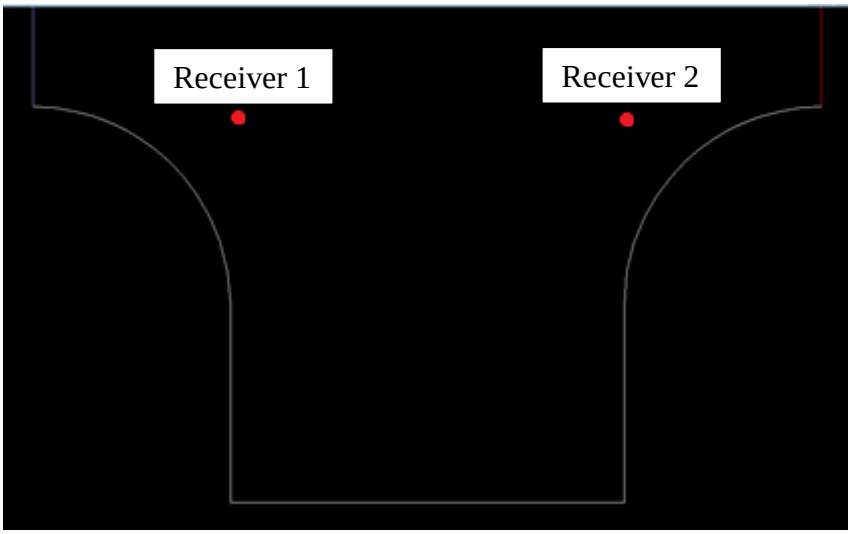

Figure 3.14: Locations of Acoustic Receivers

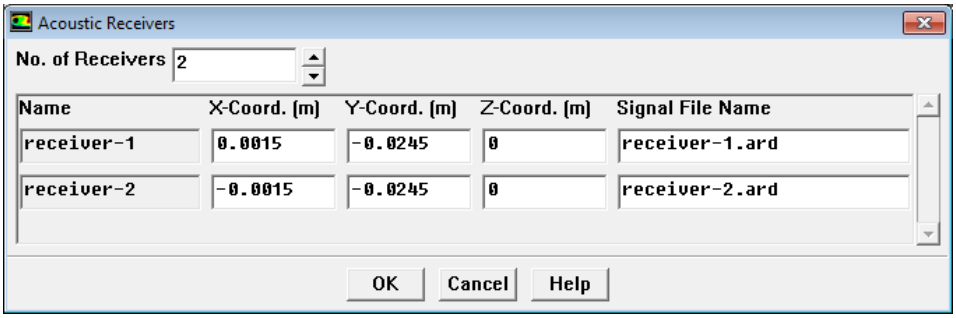

Figure 3.15: Positions of Acoustic Receivers in A Typical Geometry

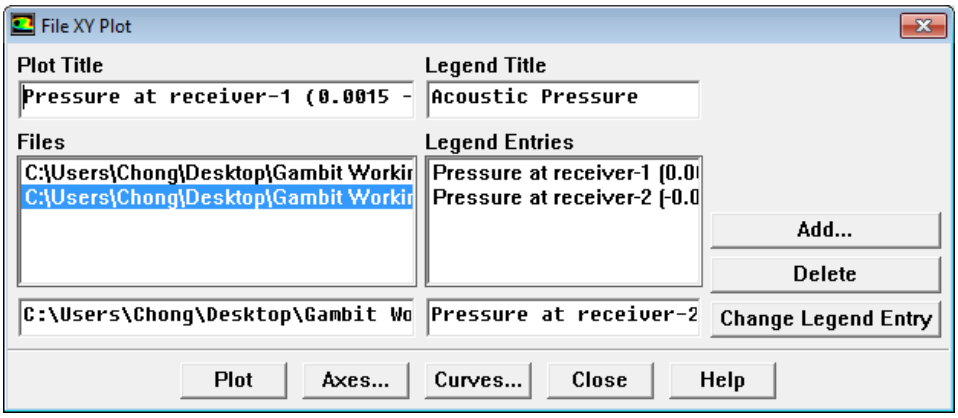

Figure 3.16: Addition of Acoustic Receivers to File XY Plot

With all the foregoing procedures completed, it is then possible to collect the acoustics data such as sound pressure level at different frequencies and different Strouhal number. From the results obtained, the Sr_{p-w} and the whistling amplitude can be determined.

In the following chapter, all the results are obtained by using an air velocity of 13.61m/s unless otherwise specified. There are two important considerations in order to read off the Sr_{p-w} from the graph obtained. Firstly, when the lock-on frequency is changed, a system will go through a minimum of energy according Popescu et al. (2011). Therefore, the peak should only be read off after the first global minimum amplitude. Secondly, the Sr_{p-w} should only be referred to the first global peak after the first global minimum amplitude.

CHAPTER 4

RESULTS AND DISCUSSION

4.1 Benchmarking and Flow Patterns of Fluid

In the following sections, the characteristic dimension used to conduct the simulation is the summation of cavity width, W and upstream edge radius, r_{up}. Nevertheless, 3 different types of characteristic dimensions including $W + r_{up}$, W and $\frac{I^2}{W+r_{up}}$ are used in Section 4.3 to determine the optimal characteristic dimension. In order to prevent confusion, Sr_{p-w} are represented in $Sr_{W+r_{up}}$, Sr_W and $Sr_{\frac{I^2}{W+r_{up}}}$ respectively, according to the characteristic dimension used to calculate the Strouhal number.

4.1.1 Benchmarking

In order to ensure the simulation results obtained from the simulation software are reliable, several bench markings have been made by comparing the simulation results with the experimental work of Nakiboğlu et al. (2010). Through the bench marking, it is found that the simulation results agree fairly well with the experimental results. Hence, the simulation method is reliable and is suitable to be used in this project as the analytical tool. As shown in Table 4.1 is the comparison of experimental results of Sr_{p-w} by Nakiboğlu et al. (2010) and the simulation results of Sr_{p-w}.

Table 4.1: Comparison of Experimental Results and Simulation Results of Sr_{p-w}.

Sample	W (mm)	H (mm)	r_{up} (mm)	r_{down} (mm)	I (mm)	Experimental Sr_{W+rup}	Simulation Sr_{W+rup}
Geo 2	4	4	2	2	4	0.36	0.34
Geo 4	4	4	2	2	0	0.38	0.35
Geo 5	4	4	2	2	8	0.40	0.40

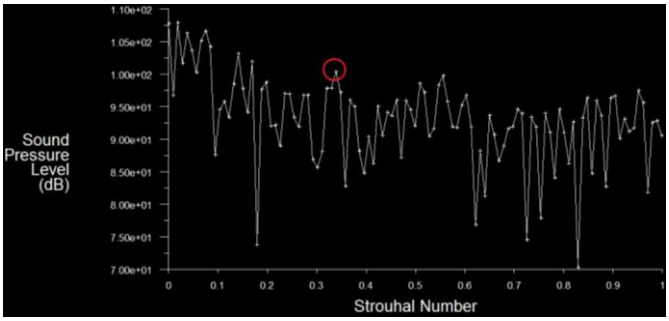

Figure 4.1: Sound Pressure Level as a Function of Strouhal Number of Geo 2 Corrugated Pipe

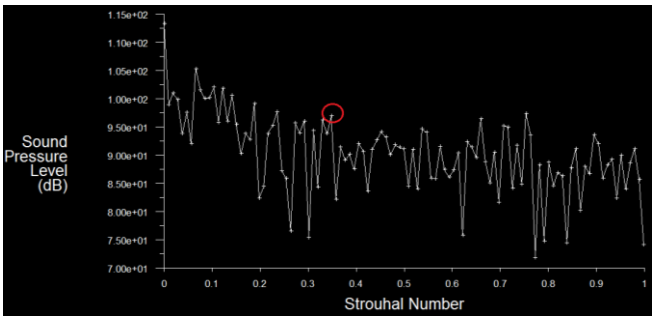

Figure 4.2: Sound Pressure Level as a Function of Strouhal Number of Geo 4 Corrugated Pipe

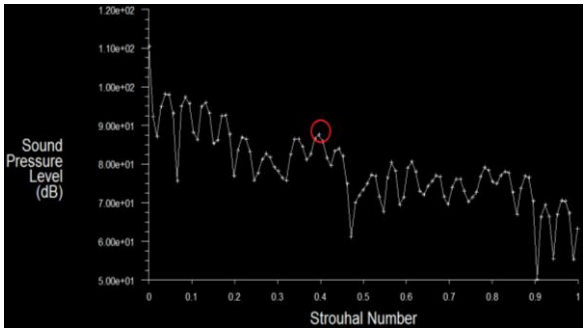

Figure 4.3: Sound Pressure Level as a Function of Strouhal Number of Geo 5 Corrugated Pipe

4.1.2 Flow Patterns of Fluid

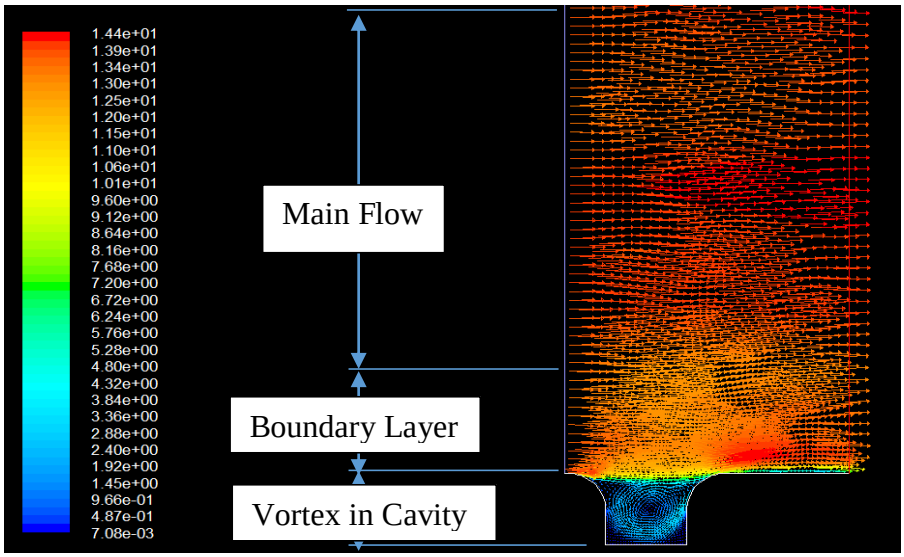

Figure 4.4: Flow Pattern of Fluid of Geo 4

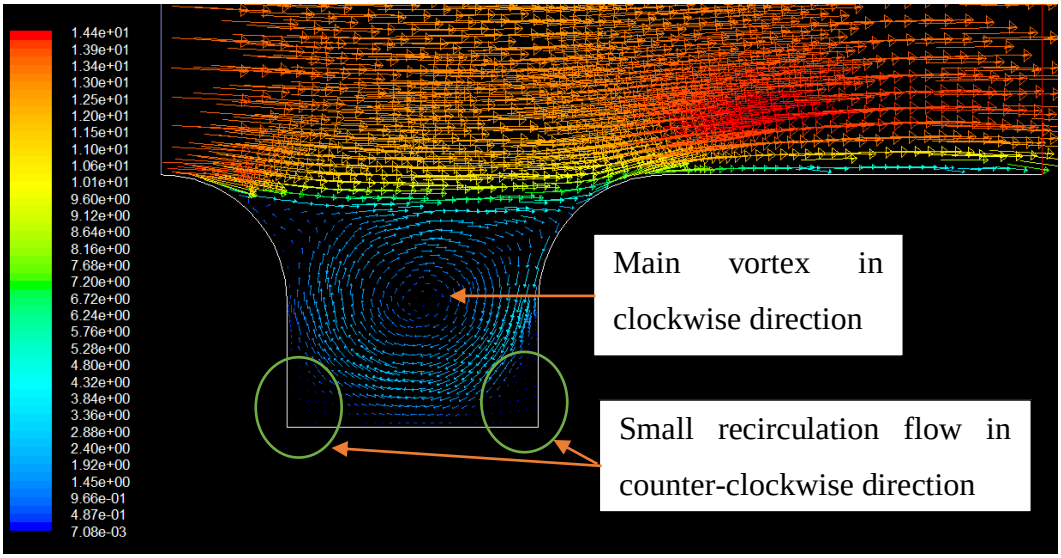

Figure 4.5: Boundary Layer and Velocity Magnitude of Vortex for Geo 4

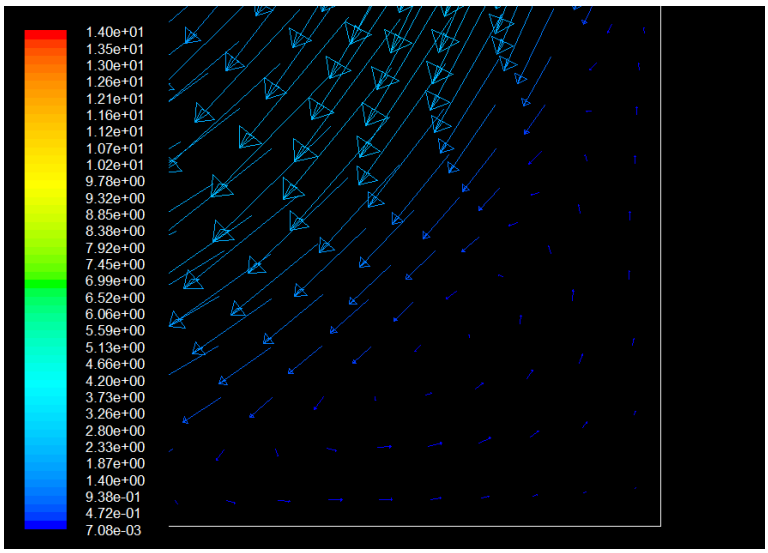

Figure 4.6: Small Recirculation Flow in Counter-clockwise Direction

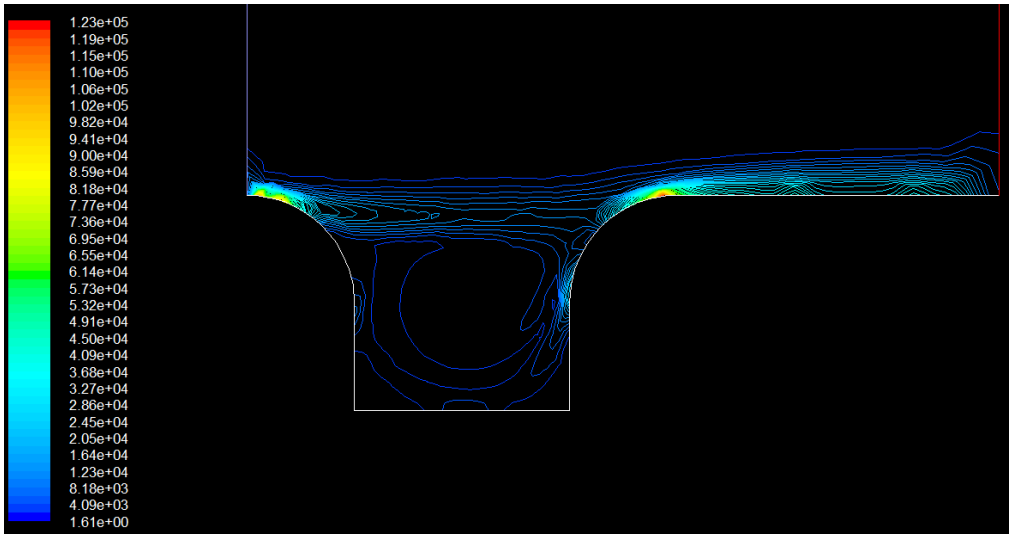

Figure 4.7: Vorticity Magnitude of Vortex for Geo 4

Figure 4.4 shows that the flow in corrugated pipe can be divided into three main regions which are main flow, boundary layer and vortices in the cavity. The main flow has uniform velocity from inlet to outlet and is unaffected by the vortex in the cavity. The boundary layer which is also known as shear layer, divides the high speed main flow region from the low speed flow region next to the pipe wall. As mentioned, the formation of shear layer is normally noticed in a turbulent flow where the viscous sublayer adjacent to the wall does not have sufficient kinetic energy to travel against an adverse pressure gradient. When this occurs, there will be a back flow along the pipe wall in the opposite direction to the main flow. Eventually, a separation of the boundary layer (shear layer) from the pipe wall is resulted at a cavity where there is abrupt pipe widening.

The flow in the boundary layer is distorted and greatly affected by the vortex in the cavity. As shown in Figure 4.5, several vortices can be noticed in the cavity of corrugated pipe. The main vortex is rotating in clockwise direction at much higher velocity than the small recirculation flow that is rotating in counter-clockwise direction as shown in Figure 4.6. Hence, it is inferred that the Sr_{p-w} and whistling amplitude are mainly affected by the main vortex that is flowing in clockwise direction.

4.2 Effects of Different Pipe Geometries on Sr_{p-w} and Whistling Amplitude

In the following sub-sections, the effects of different pipe geometries on Sr_{p-w} and whistling amplitude are discussed through the investigation of the flow patterns of the fluid in the corrugated pipe.

4.2.1 Effect of Cavity Depth, H

Table 4.2: $\frac{I}{W+r_{up}}$ Ratio, Whistling Amplitude, $Sr_{W+r_{up}}$ at Different Cavity Depths

W (mm)	H (mm)	r_{up} (mm)	r_{down} (mm)	I (mm)	$Pitch$ (mm)	$\frac{I}{(W+r_{up})}$	dB	$Sr_{W+r_{up}}$
4	4	2	2	4	12	$\frac{2}{3}$	100.0	0.34
4	6	2	2	4	12	$\frac{2}{3}$	102.5	0.34
4	8	2	2	4	12	$\frac{2}{3}$	102.5	0.30
4	10	2	2	4	12	$\frac{2}{3}$	102.5	0.30

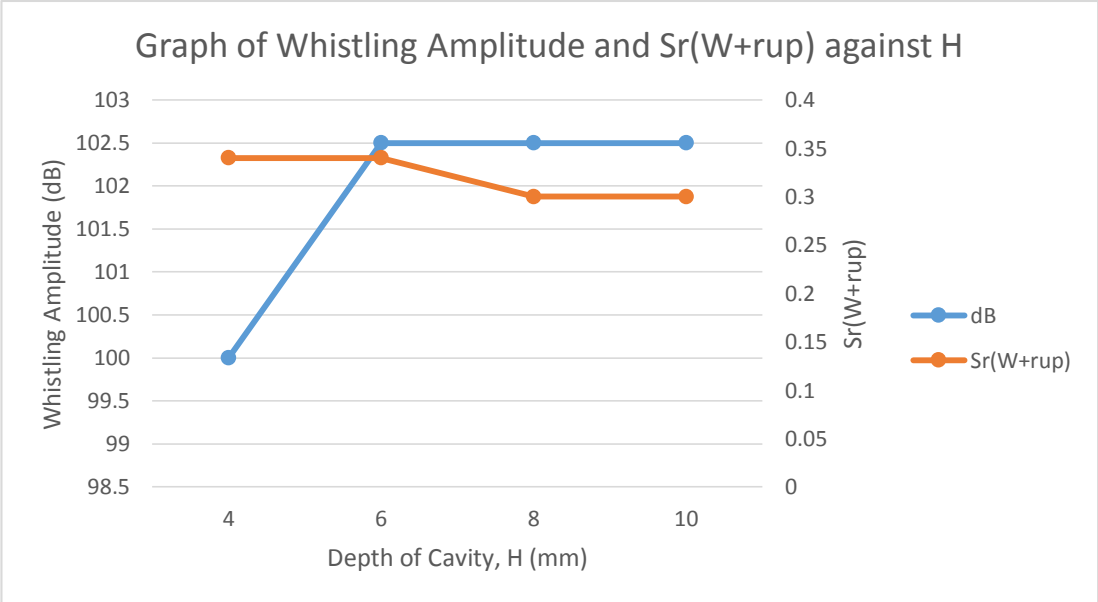

Figure 4.8: Graph of Whistling Amplitude and $Sr_{W+r_{up}}$ against H

From the results obtained from simulation (Table 4.2 and Figure 4.8), it is found that the change of cavity depth, H from 4mm to 10mm has only minor effect on the $Sr_{W+r_{up}}$. which is in the range of 0.30 to 0.34. In addition, it has also insignificant effect on the whistling amplitude which only varies between 100dB to 102.5dB. This can be inferred from the vortex velocity profile in which all the four types of geometries have similar clockwise vortex velocity magnitude around 1.5m/s even though the H is varies from 4mm to 10mm as demonstrated in Figure 4.9 and 4.10. Besides, these four geometries also shown approximately same thickness of boundary layer.

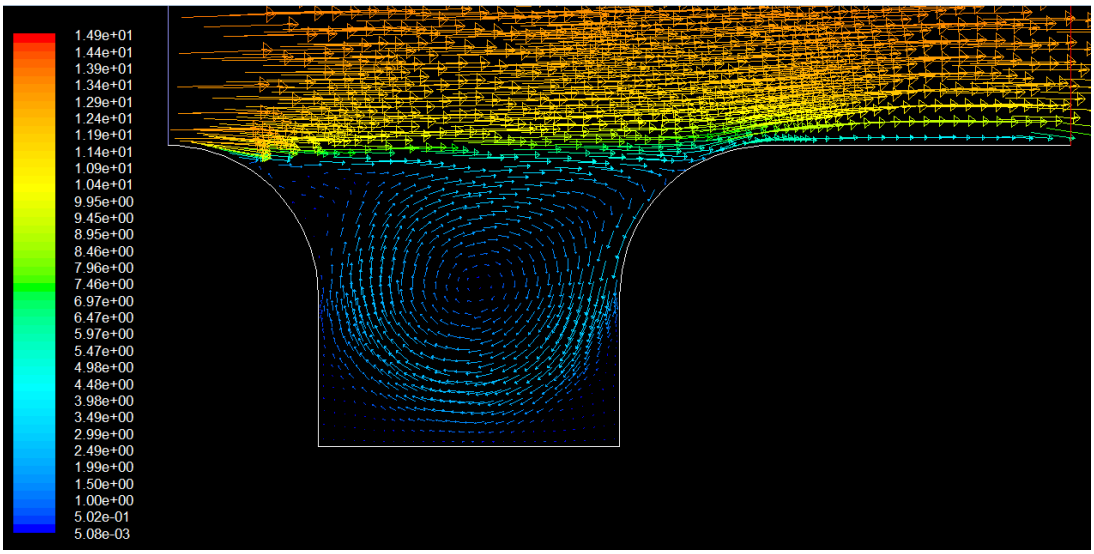

Figure 4.9: Boundary Layer and Velocity Magnitude of Vortex for Corrugated Pipe with $H = 4mm$

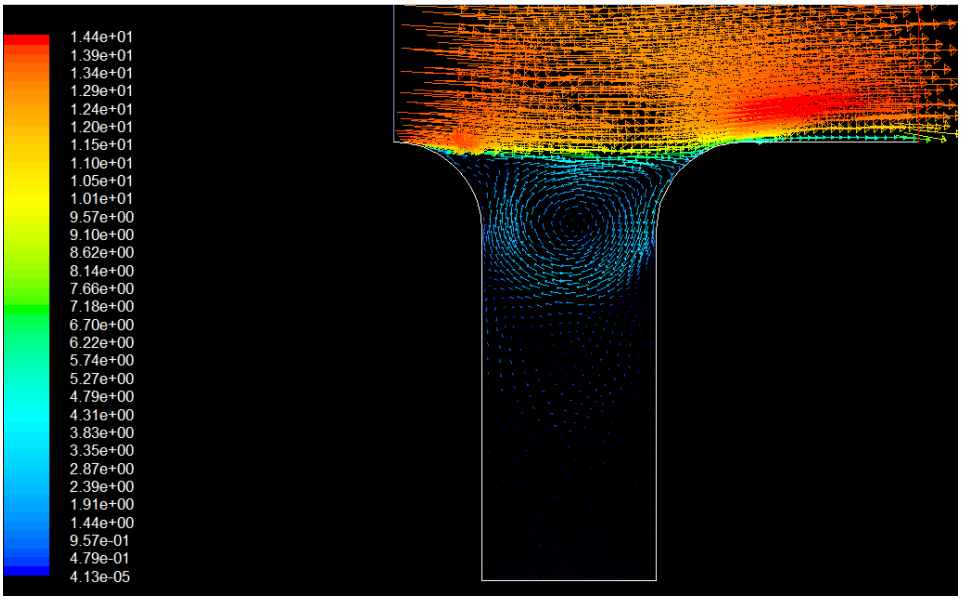

Figure 4.10: Boundary Layer and Velocity Magnitude of Vortex for Corrugated Pipe with $H = 10mm$

4.2.2 Effect of Downstream Edge Radius, r_{down}

Table 4.3: $\frac{I}{W+r_{up}}$ Ratio, Whistling Amplitude, $Sr_{W+r_{up}}$ at Different Downstream Edge Radius

W (mm)	H (mm)	r_{up} (mm)	r_{down} (mm)	I (mm)	$Pitch$ (mm)	$\frac{I}{(W+r_{up})}$	dB	$Sr_{W+r_{up}}$
4	4	2	2	2	10	$\frac{1}{3}$	103.8	0.15
4	4	2	4	2	12	$\frac{1}{3}$	101.3	0.20
4	6	2	6	2	14	$\frac{1}{3}$	107.0	0.24
4	8	2	8	2	16	$\frac{1}{3}$	102.0	0.16
4	10	2	10	2	18	$\frac{1}{3}$	102.0	0.11

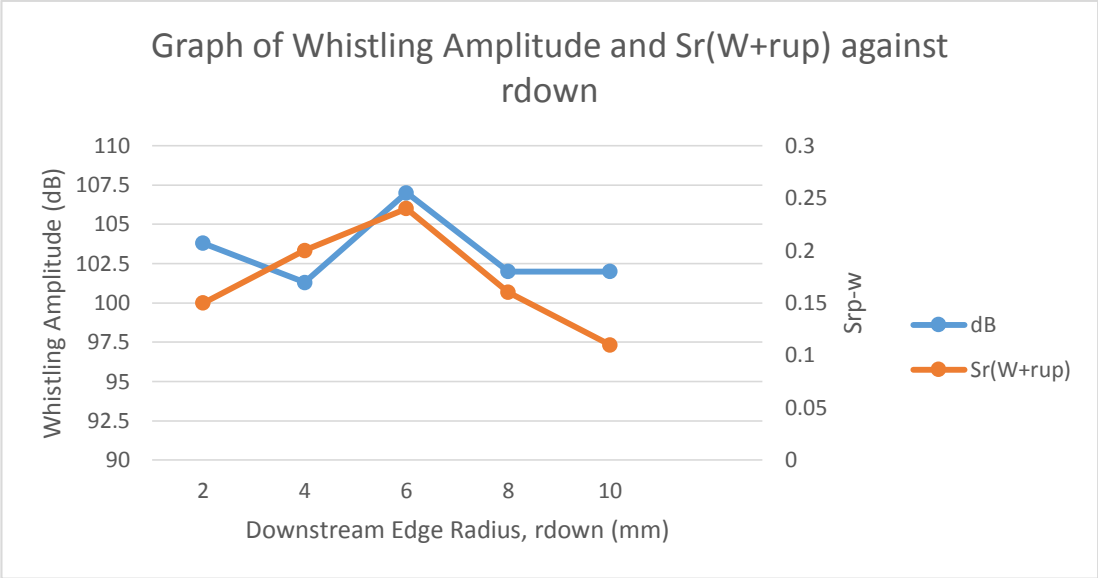

Figure 4.11: Graph of Whistling Amplitude and $Sr_{W+r_{up}}$ against r_{down}

The change of downstream edge radius, r_{down} from 2mm to 10mm has varied the $Sr_{W+r_{up}}$ within the range of 0.11 to 0.24, which is very minor. On the other hand, the change of r_{down} does not affect the whistling amplitude greatly. The largest difference of whistling amplitude is only 5.7dB. The results is agreed with the work of Nakiboğlu et al. (2010) who explained that this is because the shear layer thickness has become less concentrated as the downstream edge is approached. This can also be explained by the small changes of clockwise vortex velocity magnitude from 1.43m/s to 1.52m/s as r_{down} is varied. As demonstrated in Figure 4.12 and Figure 4.13, the vortex velocity in two geometries are similar even though their r_{down} varies significantly.

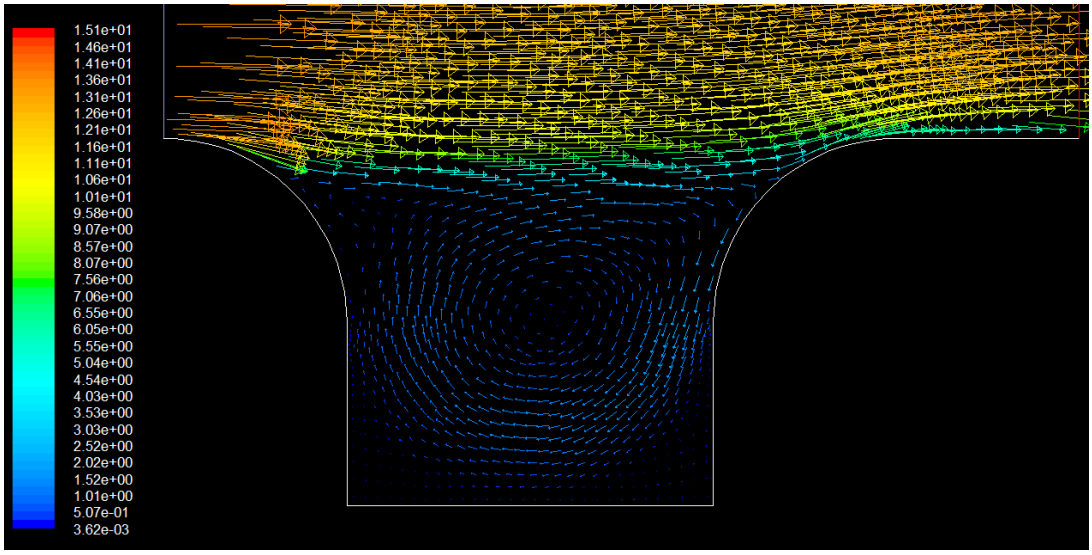

Figure 4.12: Boundary Layer and Velocity Magnitude of Vortex for Corrugated Pipe with $r_{down} = 2mm$

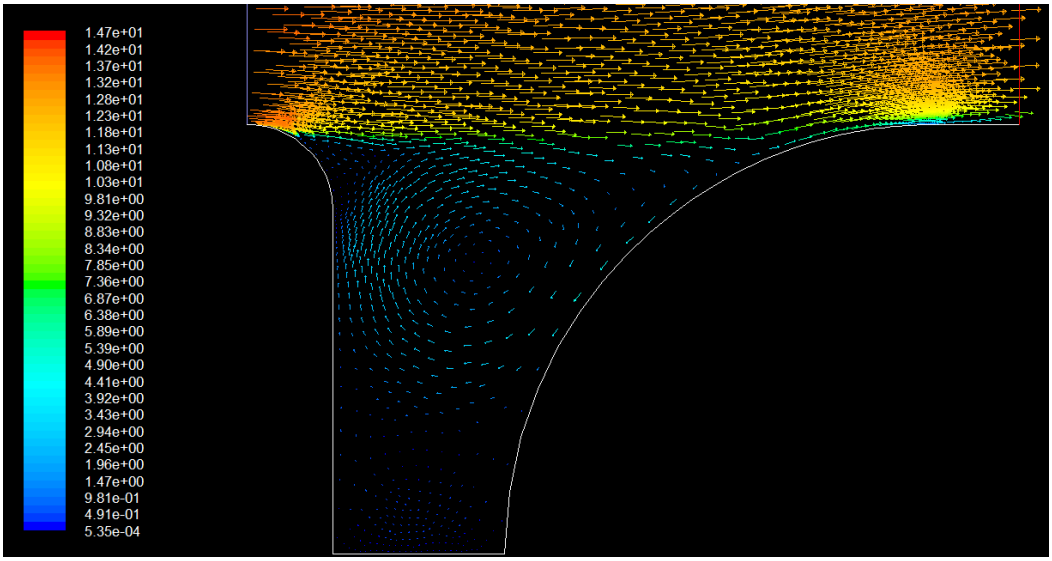

Figure 4.13: Boundary Layer and Velocity Magnitude of Vortex for Corrugated Pipe with $r_{down} = 10mm$

4.2.3 Effect of Upstream Edge Radius, r_{up}

Table 4.4: $\frac{I}{W+r_{up}}$ Ratio, Whistling Amplitude, $Sr_{W+r_{up}}$ at Different Upstream Edge Radius

W (mm)	H (mm)	r_{up} (mm)	r_{down} (mm)	I (mm)	$Pitch$ (mm)	$\frac{I}{(W+r_{up})}$	dB	$Sr_{W+r_{up}}$
4	4	2	2	2	10	$\frac{1}{3}$	103.8	0.15
4	4	4	2	2	12	$\frac{1}{4}$	97.0	0.37
4	6	6	2	2	14	$\frac{1}{5}$	95.0	0.57
4	8	8	2	2	16	$\frac{1}{6}$	92.5	0.62
4	10	10	2	2	18	$\frac{1}{7}$	93.0	0.42

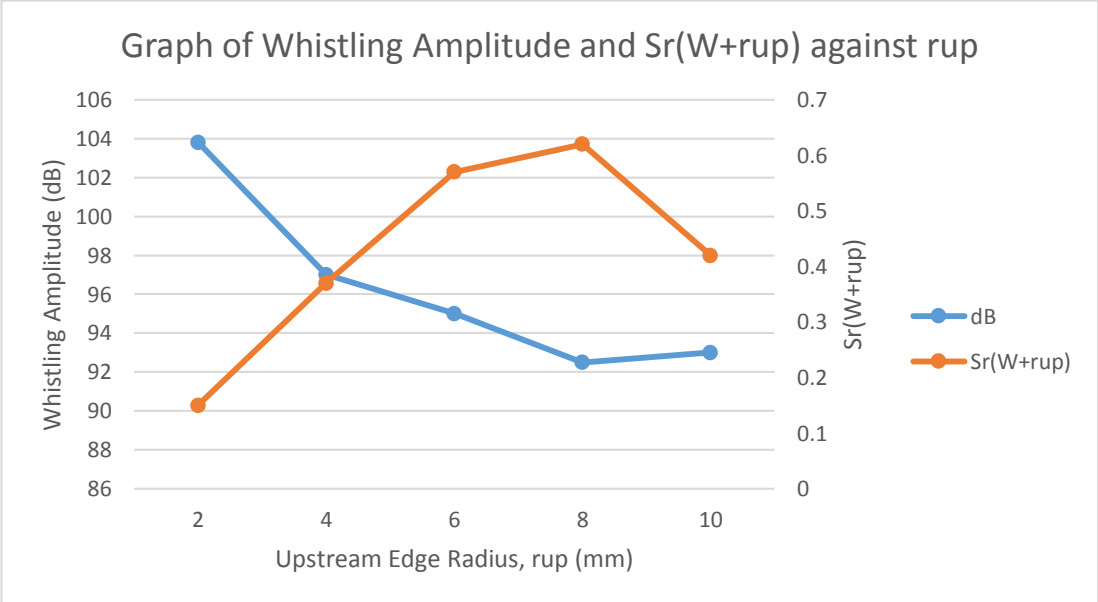

Figure 4.14: Graph of Whistling Amplitude and $Sr_{W+r_{up}}$ against r_{up}

From Table 4.4 and Figure 4.14, it is observed that as the upstream edge radius, $r_{up}$is increased from 2mm to 8mm, the $Sr_{W+r_{up}}$is increased from 0.15 to 0.62.

When r_{up} is further increased to 10mm, the $Sr_{W+r_{up}}$ is dropped to 0.42. Nothing can be concluded so far in terms of the effect of r_{up} to $Sr_{W+r_{up}}$. On the other hand, it is observed from the velocity profile that the boundary layer becomes thinner and the clockwise vortex becomes weaker as the r_{up} is increased. For instance, the vortex velocity in the cavity with $r_{up} = 2mm$ as shown in Figure 4.15 (2.52m/s) is much stronger than the vortex velocity in the cavity with $r_{up} = 10mm$ as shown in Figure 4.16 (1.49m/s). This can therefore explain why the whistling amplitude is decreased as the r_{up} is increased until a saturation is observed at r_{up} of 8mm. There is a reduction of 11.3dB when r_{up} is increased from 2mm to 8mm. The results are also in agreement with (Nakiboğlu et al., 2010) who discovered that rounding of upstream edge radius of cavity (r_{up}) is able to reduce the initial sound absorption and increase the whistling amplitude by a factor of 3 to 5.

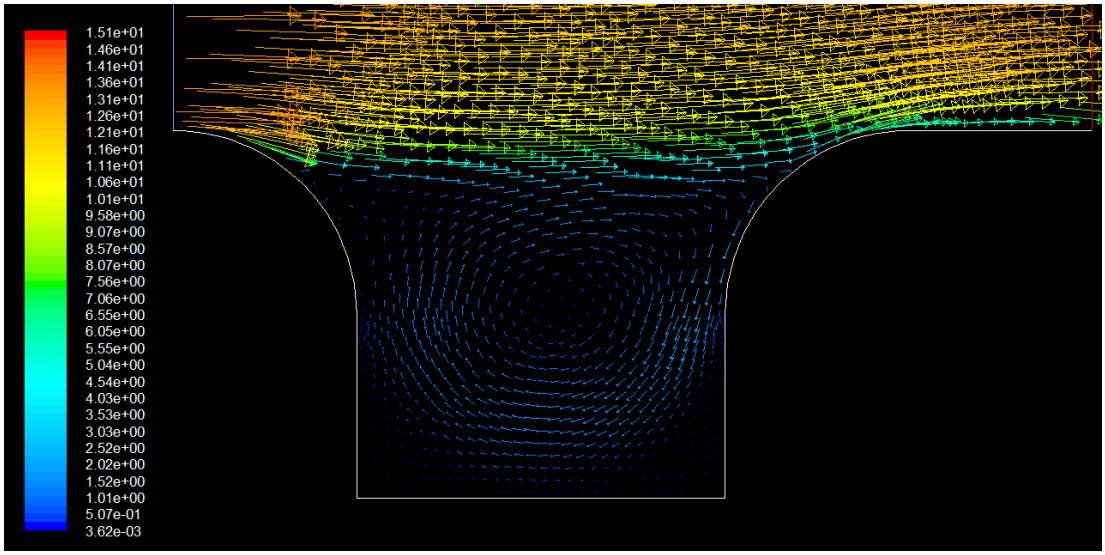

Figure 4.15: Boundary Layer and Velocity Magnitude of Vortex for Corrugated Pipe with $r_{up} = 2mm$

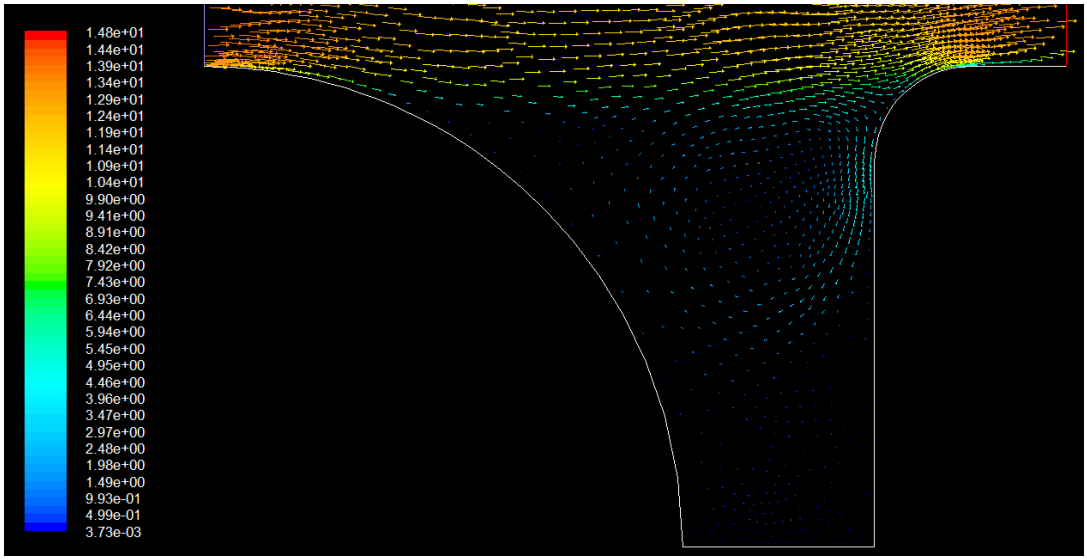

Figure 4.16: Boundary Layer and Velocity Magnitude of Vortex for Corrugated Pipe with $r_{up} = 10mm$

4.2.4 Effect of Cavity Width, W

Table 4.5: $\frac{I}{W+r_{up}}$ Ratio, Whistling Amplitude, $Sr_{W+r_{up}}$ at Different Cavity Widths

W (mm)	H (mm)	r_{up} (mm)	r_{down} (mm)	I (mm)	$Pitch$ (mm)	$\frac{I}{(W+r_{up})}$	dB	$Sr_{W+r_{up}}$
2	4	2	2	2	8	$\frac{1}{2}$	107.5	0.30
4	4	2	2	2	10	$\frac{1}{3}$	103.8	0.15
6	4	2	2	2	12	$\frac{1}{4}$	92.5	0.31
8	4	2	2	2	14	$\frac{1}{5}$	89.0	0.58
10	4	2	2	2	16	$\frac{1}{6}$	84.0	0.57
12	4	2	2	2	18	$\frac{1}{7}$	83.0	0.44

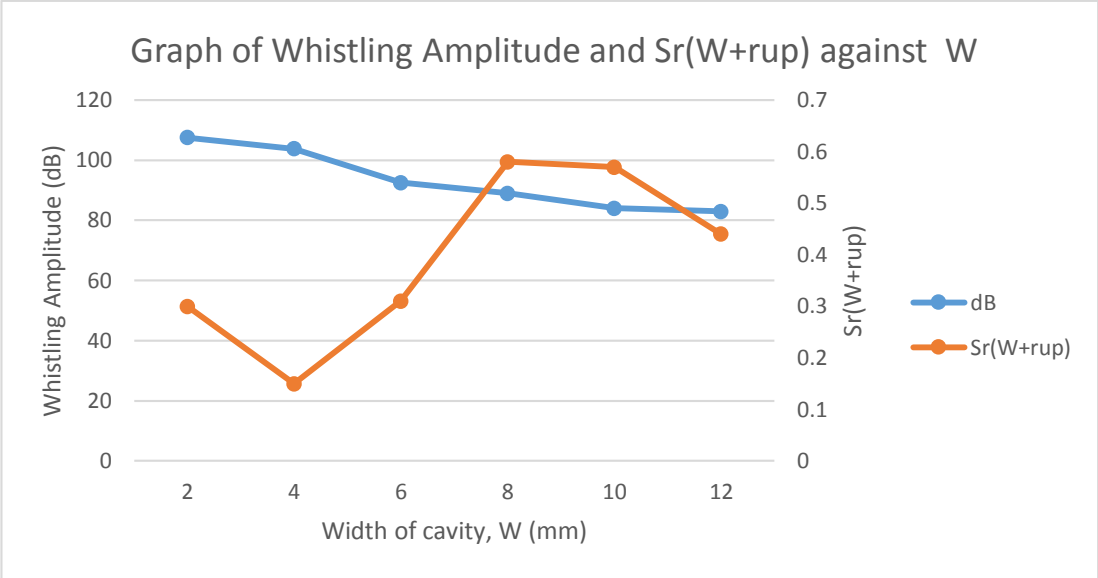

Figure 4.17: Graph of Whistling Amplitude and $Sr_{W+r_{up}}$ against W

When the width of the cavity, W is changed, a similar observation is noted as to that of the change of r_{up}. There is no a clear relationship between W and $Sr_{W+r_{up}}$ because the $Sr_{W+r_{up}}$ fluctuates as the W is changed. On the other hand, although thicker boundary layer and stronger clockwise vortex are observed, the whistling amplitude is reduced significantly as the W is increased. As seen in Table 4.5 and Figure 4.17, the whistling amplitude is reduced from 107.5dB to 83dB when W is increased from 2mm to 12mm. A closer investigation to the vortex profile reveals that a secondary counter-clockwise vortex is formed at the upstream of the primary clockwise vortex when W is 6mm and 8mm. Besides, a tertiary clockwise vortex is also formed at the upstream of the secondary counter-clockwise vortex when W is 10mm and 12mm. It is inferred that these secondary and tertiary vortices are contributing to the reduction of whistling amplitude through a "cancelling" effect to the primary vortex. The secondary vortex can be observed in Figure 4.19 and both secondary and tertiary vortices can be observed in Figure 4.20.

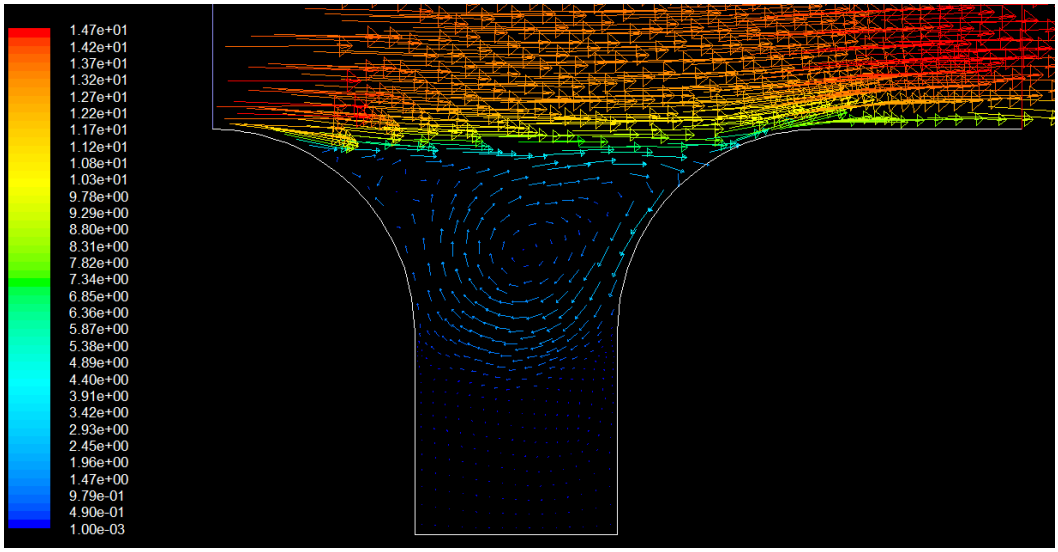

Figure 4.18: Boundary Layer and Velocity Magnitude of Vortex for Corrugated Pipe with $W = 2mm$

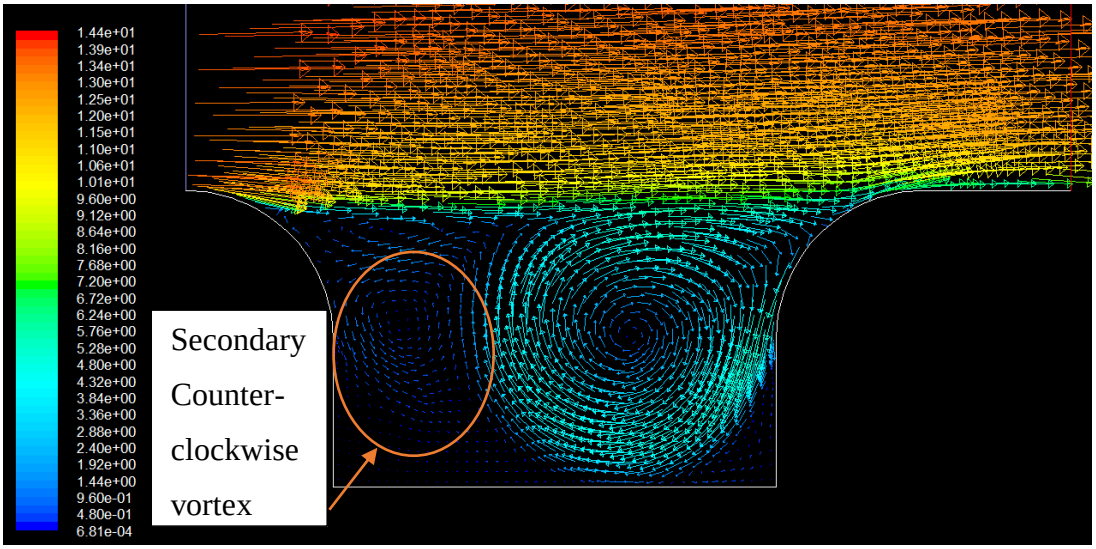

Figure 4.19: Boundary Layer and Velocity Magnitude of Vortex for Corrugated Pipe with $W = 6mm$

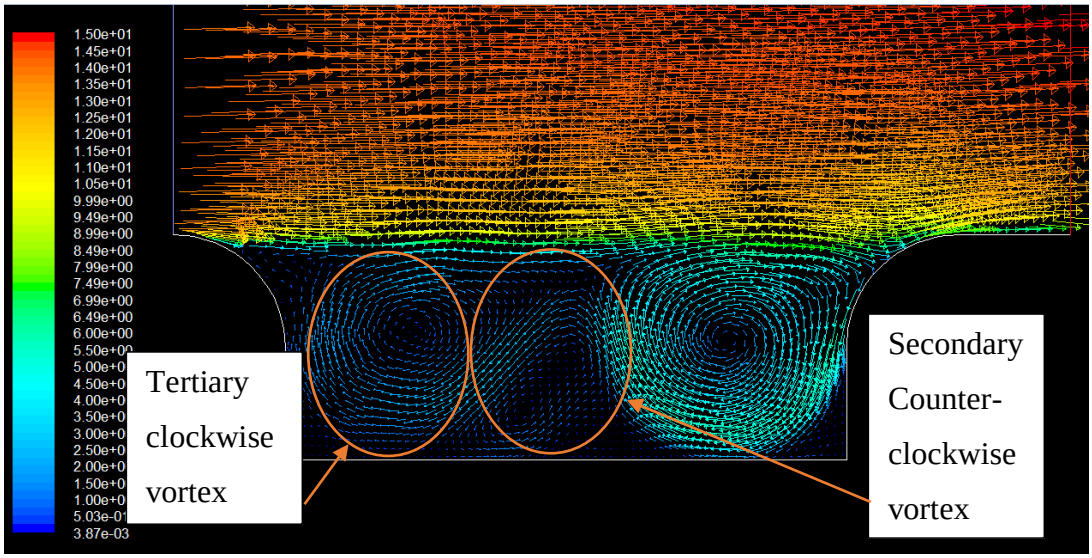

Figure 4.20: Boundary Layer and Velocity Magnitude of Vortex for Corrugated Pipe with $W = 10mm$.

4.2.5 Effect of Plateau, I

Table 4.6: $\frac{I}{W+r_{up}}$ Ratio, Whistling Amplitude, $Sr_{W+r_{up}}$ at Different Plateaus

W (mm)	H (mm)	r_{up} (mm)	r_{down} (mm)	I (mm)	$Pitch$ (mm)	$\frac{I}{(W+r_{up})}$	dB	$Sr_{W+r_{up}}$
4	4	2	2	0	8	0	97.0	0.35
4	4	2	2	2	10	$\frac{1}{3}$	103.8	0.15
4	4	2	2	3	11	$\frac{1}{2}$	72.0	0.28
4	4	2	2	4	12	$\frac{2}{3}$	100.0	0.34
4	4	2	2	5	13	$\frac{5}{6}$	99.0	0.27
4	4	2	2	6	14	1	83.0	0.39
4	4	2	2	7	15	$\frac{7}{6}$	97.5	0.39
4	4	2	2	8	16	$\frac{4}{3}$	87.5	0.40

4	4	2	2	9	17	$\frac{3}{2}$	96.3	0.40
4	4	2	2	10	18	$\frac{5}{3}$	92.0	0.43

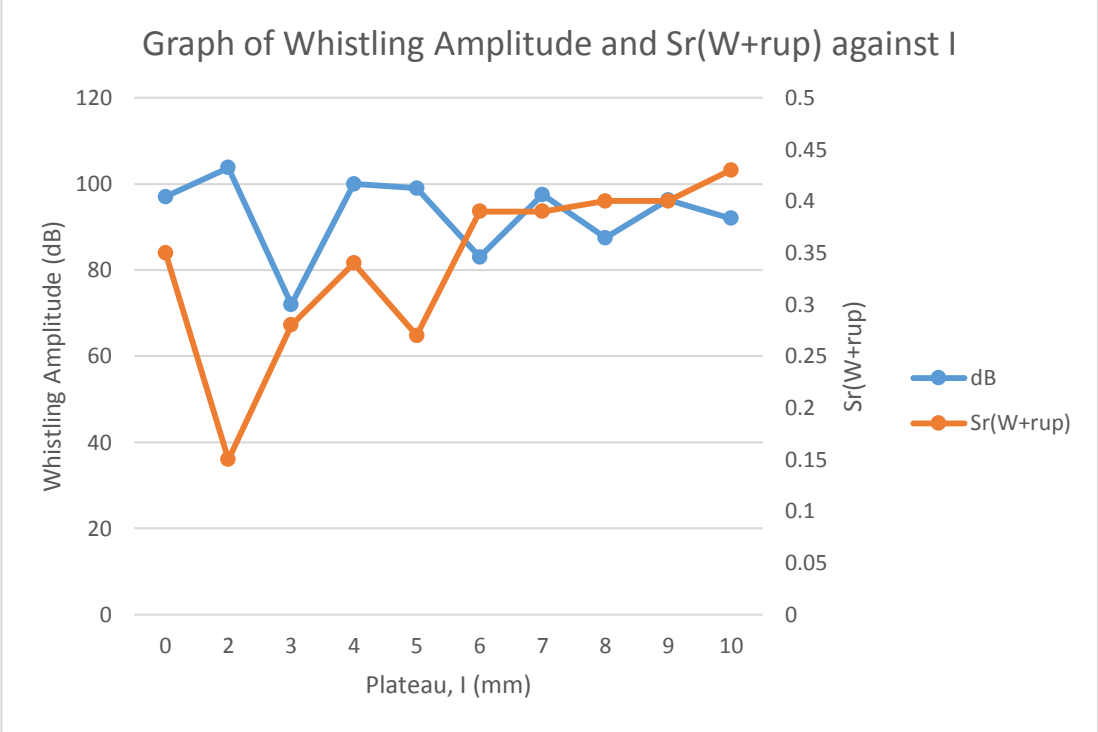

Figure 4.21: Graph of Whistling Amplitude and $Sr_{W+r_{up}}$ against l

From Table 4.6 and Figure 4.21, it is found that the whistling amplitude does not show an explicit trend as plateau, I is changed. According to Nakiboğlu and Hirschberg (2012), there is a shift of peaks as I is varied. In other words, a secondary peak will form and grow at certain plateau length to replace the first peak which diminishes in the process until it disappears. Furthermore, an important finding is observed from Table 4.6. It is noted that the $Sr_{W+r_{up}}$ fluctuates when I is varied from 0mm to 6mm. Nevertheless, the $Sr_{W+r_{up}}$ becomes more constant as I is changed from 6mm to 10mm.

The value of 6mm is exactly the same as the summation of W and r_{up} $(W + r_{up})$. Therefore, it is inferred that there is a relationship between the I and $(W + r_{up})$.

In order to investigate this relationship, the ratio of $\frac{I}{W+r_{up}}$ is computed for every geometry from Table 4.2 to Table 4.6 and tabulated in Figure 4.22.

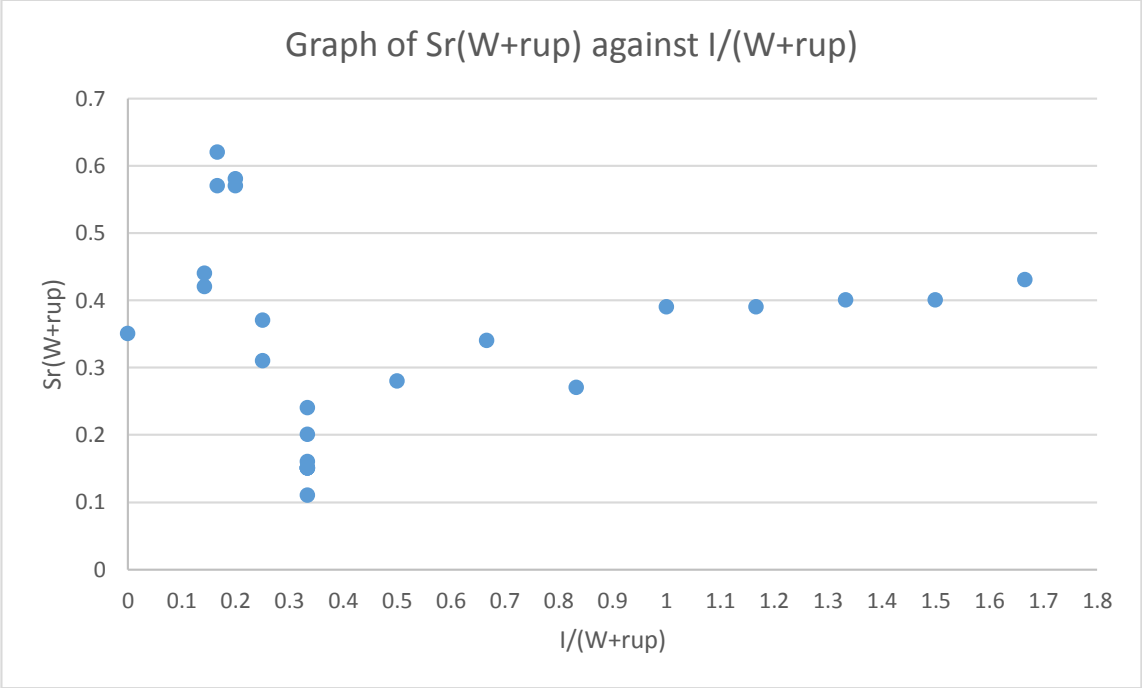

Figure 4.22: Graph of $Sr_{W+r_{up}}$ against $\frac{I}{W+r_{up}}$

From Figure 4.22, it is observed that when $I < W + r_{up}$, the value of $Sr_{W+r_{up}}$ is fluctuating. $Sr_{W+r_{up}}$ is at a maximum value of 0.62 when $\frac{I}{W+r_{up}}$ is 0.1667 and at a minimum value of 0.11 to 0.24 when $\frac{I}{W+r_{up}}$ is 0.3333. There is a smaller fluctuation for $0.3333 < \frac{I}{W+r_{up}} < 1$.

Nevertheless, when $I \geq W + r_{up}$ or $\frac{I}{W+r_{up}} \geq 1$, the value of $Sr_{W+r_{up}}$ is far more constant in the range of 0.39 to 0.43. A conclusion that can be made at this point is that when $I < W + r_{up}$, W and r_{up} have dominant effect over I in affecting the flow over corrugated pipe, therefore the value of $Sr_{W+r_{up}}$ is fluctuating. However, when $I \geq W + r_{up}$, I is dominant over W and r_{up}. The change of $Sr_{W+r_{up}}$ in this range is

insignificant, which means that I does not contribute much to the change of $Sr_{W+r_{up}}$ as compared to W and r_{up} as discussed earlier.

Although the ratio of $\frac{I}{W+r_{up}}$ is a good indicator of the consistency of $Sr_{W+r_{up}}$, it cannot be used to infer the value of $Sr_{W+r_{up}}$. In other words, even though two corrugated geometries have the same ratio of $\frac{I}{W+r_{up}}$, they do not necessary have the same value of $Sr_{W+r_{up}}$. This can be seen by comparing Table 4.6 and 4.7. Although some of the geometries in two tables have the same ratio of $\frac{I}{W+r_{up}}$, their $Sr_{W+r_{up}}$ are significantly different.

It should be noted that Table 4.7 also shows a similar phenomenon as mentioned earlier, where a consistency of value of $Sr_{W+r_{up}}$ is observed when $I \geq W + r_{up}$ or $\frac{I}{W+r_{up}} \geq 1$.

Table 4.7: $\frac{I}{W+r_{up}}$ Ratio, Whistling Amplitude, $Sr_{W+r_{up}}$ at Different Geometries

W (mm)	H (mm)	r_{up} (mm)	r_{down} (mm)	I (mm)	$Pitch$ (mm)	$\frac{I}{(W+r_{up})}$	dB	$Sr_{W+r_{up}}$
11	6	6	2	10	42	$\frac{10}{17}$	88.8	0.67
11	4	4	2	10	27	$\frac{2}{3}$	98.8	0.28
6	4	4	2	10	22	1	97.0	0.21
4.5	4	3	2	10	19.5	$\frac{4}{3}$	104.0	0.22
4.5	4	1.5	2	10	18	$\frac{5}{3}$	94.0	0.17

4.3 Optimal Characteristic Dimension

4.3.1 Determination of Optimal Characteristic Dimension

Numerous works have been done previously to determine the optimal characteristic dimension and the sum of the width of cavity and the upstream edge radius, $W + r_{up}$, which is also known as modified gap width, is found to be the best representation of characteristic dimension. Since the ratio of $\frac{I}{W+r_{up}}$ is found to be a good indicator of the consistency of $Sr_{W+r_{up}}$, it is therefore possible to use it as a characteristic dimension in calculating the Strouhal number provided it can give a lesser variation of Sr_{p-w} than the use of $W + r_{up}$ as characteristic dimension.

Nevertheless, $\frac{I}{W+r_{up}}$ is only a ratio but not a length. It cannot be used as a characteristic dimension unless it has a unit of meter. In order to make it a characteristic dimension with unit of meter, $\frac{I^2}{W+r_{up}}$ is proposed in this project. This parameter is verified to be a good indicator of the consistency of $Sr_{W+r_{up}}$as a similar pattern in Figure 4.23 is also observed in Figure 4.22, in which the $Sr_{W+r_{up}}$is plotted against $\frac{I^2}{W+r_{up}}$.

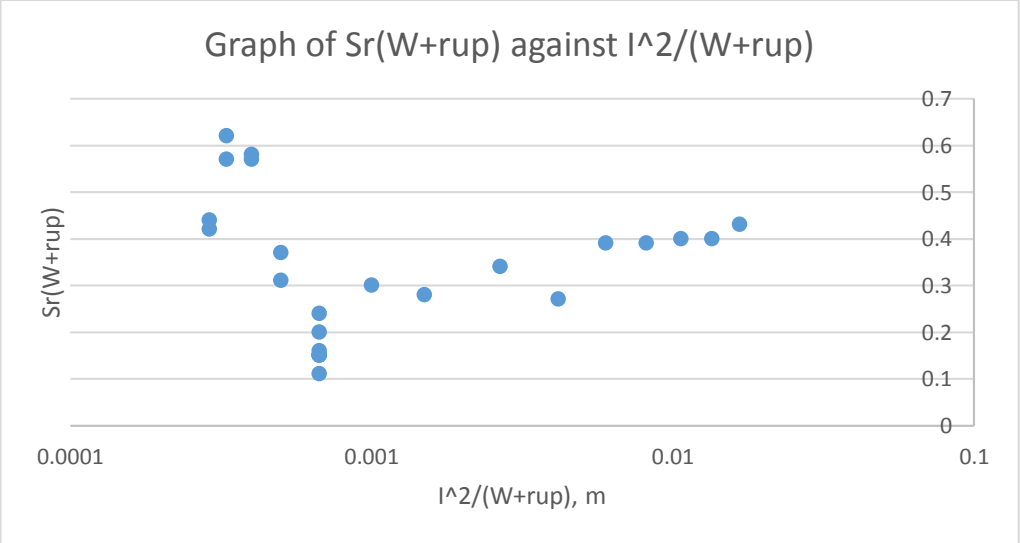

Figure 4.23: Graph of $Sr_{W+r_{up}}$against $\frac{I^2}{W+r_{up}}$

Furthermore, W is also used as a characteristic dimension in this paper and the results of Sr_{p-w} obtained by using air velocity from 11.61m/s to 21.61m/s for three different types of characteristic dimensions are tabulated in Table 4.8.

Table 4.8: $Sr_{W+r_{up}}$, Sr_W and $Sr_{\frac{I^2}{W+r_{up}}}$ at Different Geometries

W (mm)	H (mm)	r_{up} (mm)	r_{down} (mm)	I (mm)	$Pitch$ (mm)	$Velocity$ $\left(\frac{m}{s}\right)$	$Sr_{W+r_{up}}$	Sr_W	$Sr_{\frac{I^2}{W+rup}}$
4	4	2	2	4	12	11.61	0.38	0.29	0.10
4	4	2	2	4	12	13.61	0.34	0.25	0.05
4	4	2	2	4	12	15.61	0.30	0.20	0.13
4	4	2	2	4	12	17.61	0.30	0.09	0.06
4	4	2	2	4	12	19.61	0.43	0.17	0.08
4	4	2	2	4	12	21.61	0.30	0.08	0.05

From Table 4.8, it is observed that the use of $W + r_{up}$ as the characteristic dimension results in variation of Strouhal number of $0.30 \leq Sr_{W+r_{up}} \leq 0.43$. The use of W as the characteristic dimension has led to larger variation of Strouhal number in the range of $0.09 \leq Sr_W \leq 0.29$. The smallest variation in Strouhal number is observed when $\frac{I^2}{W+r_{up}}$ is used as the characteristic dimension, which is limited to $0.05 \leq Sr_{\frac{I^2}{W+r_{up}}} \leq 0.13$.

It is therefore proven that $\frac{I^2}{W+r_{up}}$ is a better characteristic dimension than $W + r_{up}$ as the use of $\frac{I^2}{W+r_{up}}$ in the calculation of Strouhal number led to smallest variation. This finding is significant as it can allow a better design of flow condition to minimize and avoid the whistling phenomenon. The equation 1.1 can be rearranged to obtain the following formula:

$$U_{cr} = \frac{f_n L_c}{Sr_{p-w}} \quad (4.1)$$

where

f_n = acoustic natural frequency of the pipe, Hz

L_c = characteristic dimension, m

U_{cr} = critical flow velocity in the pipe, m/s

$Sr_{p\text{-}w}$ = peak whistling Strouhal number

This formula can allow us to predict the critical flow condition in which whistling phenomenon will occur and therefore avoid it. The value of Sr_{p-w} can be obtained from the data obtained from the simulations when a particular value of characteristic dimension $\left(\frac{I^2}{W+r_{up}}\right)$ is selected. The acoustic natural frequency of the pipe, f_n can then be calculated by using Cumming's formula as proposed in Kristiansen and Wiik (2006) for corrugated pipe as follow:

$$f_n = 0.89\frac{nc}{2L'} \quad (4.2)$$

where

n = mode number (1, 2, 3, ….)

c = speed of sound, m/s

L' = effective pipe length, m

When the critical flow velocity, U_{cr} has been determined, it can be easily avoided by manipulating the fluid flow velocity. It is also possible to select or design the parameters of the corrugated pipe if the flow velocity cannot be manipulated.

For instance, given a 2m long corrugated pipe and speed of sound of 340.29m/s, the second mode of acoustic natural frequency is calculated to be 151.43Hz by using equation 4.2. If the $Sr_{\frac{I^2}{W+r_{up}}}$ is found to be 0.1 from the simulation for the pipe with $\frac{I^2}{W+r_{up}}$ of 0.005, the U_{cr} can then be determined to be around 7.57m/s from equation 4.1. In order to avoid whistling phenomenon, the flow condition should be

much larger or smaller than this value. It is important to note that other modes of resonance frequency should also be calculated and avoided accordingly.

In the cases where flow velocity is constant, equation 4.1 can also be used. For instance, if a 2m corrugated pipe with $I = 8mm$, $W = 10mm$ and $r_{up} = 2.8mm$ with second mode of acoustic natural frequency of 151.43Hz (calculated using equation 4.2) is selected for a flow condition of 8m/s, its $Sr_{\frac{I^2}{W+r_{up}}}$ can be determined with equation 4.1 to be around 0.0946. This value is then compared with simulation method by using $\frac{I^2}{W+r_{up}}$ of 0.005. If the values of $Sr_{\frac{I^2}{W+r_{up}}}$ is different between calculated value and simulation results, this particular design of corrugated pipe is suitable to be used for the flow condition. However, a different pipe should be re-selected shall the values of $Sr_{\frac{I^2}{W+r_{up}}}$ is similar or same between calculated value and simulation results. With the proposed method, the whistling phenomenon can be overcome effectively.

It should also be noted that the simulation method proposed in this project is able to contribute effectively in the research of flow induced acoustics in corrugated pipe. This is because the conduction of simulation is much simpler than running an experiment. Different models of corrugated pipe can be easily drawn with few minutes and simulation results can be obtained easily with high accuracy. Hence, time can be saved and the progress of research can be accelerated.

Furthermore, the use of simulation method is cheaper than the use of experimental method. This is because simulation method can provide a wide range of flow conditions and information without the need of costly experimental setup provided the initial conditions and boundary conditions are specified correctly. This can also reduce waste of material since different configurations of corrugated pipe are not required.

Last but not least, large amount of space is not required by using simulation method since no equipment are needed. This can save the cost indirectly while not compromising the accuracy of the results.

CHAPTER 5

CONCLUSION AND RECOMMENDATIONS

5.1 Conclusion

In this paper, the effects of various corrugated pipe geometries on the Sr_{p-w} and whistling amplitude are simulated using CFD software. The simulation method is first compared with the experimental results from Nakiboğlu et al. (2010) to ensure the reliability of the results obtained. The 2D numerical simulation method is found to be accurate in determining the the Sr_{p-w} and whistling amplitude.

The change of cavity depth, $H$and downstream edge radius, r_{down} are found to have insignificant effect on the Sr_{p-w} and whistling amplitude. It is found that the change of cavity depth, H from 4mm to 10mm only changes $Sr_{W+r_{up}}$ from 0.30 to 0.34. In addition, it has also insignificant effect on the whistling amplitude which only varies between 100dB to 102.5dB. The change of downstream edge radius, $r_{down}$from 2mm to 10mm has varied the $Sr_{W+r_{up}}$within the range of 0.11 to 0.24, which is very minor. On the other hand, the change of r_{down} does not affect the whistling amplitude greatly. The largest difference of whistling amplitude is only 5.7dB.

However, the increase of upstream edge radius, $r_{up}$and cavity width, Wlead to a fluctuation of Sr_{p-w} and a reduction of whistling amplitude. Whistling amplitude is dropped from 103.8dB to 93dB when r_{up} is increased from 2mm to 10mm. Besides, whistling amplitude is reduced from 107.5dB to 83dB when W is increased from 2mm to 12mm.

The strongest finding is that when $I < W + r_{up}$, the value of $Sr_{W+r_{up}}$ is fluctuating. $Sr_{W+r_{up}}$ is at a maximum value of 0.62 when $\frac{I}{W+r_{up}}$ is 0.1667 and at a minimum value of 0.11 to 0.24 when $\frac{I}{W+r_{up}}$ is 0.3333. There is a smaller fluctuation for $0.3333 < \frac{I}{W+r_{up}} < 1$.

Nevertheless, when $I \geq W + r_{up}$ or $\frac{I}{W+r_{up}} \geq 1$, the value of $Sr_{W+r_{up}}$ is far more constant in the range of 0.39 to 0.43. It can be concluded that when $I < W + r_{up}$, W and r_{up} have dominant effect over I in affecting the flow over corrugated pipe, therefore value of $Sr_{W+r_{up}}$ is fluctuating. However, when $I \geq W + r_{up}$, l is dominant over W and r_{up}. The change of $Sr_{W+r_{up}}$ in this range is insignificant, which means that I does not contribute much to the change of $Sr_{W+r_{up}}$ as compared to W and r_{up} as discussed earlier.

Since the ratio of $\frac{I}{W+r_{up}}$ is found to be a good indicator of the consistency of $Sr_{W+r_{up}}$, it is therefore possible to use it as a characteristic dimension in calculating the Strouhal number. Nevertheless, $\frac{I}{W+r_{up}}$ is only a ratio but not a length. It cannot be used as a characteristic dimension unless it has a unit of meter. In order to make it a characteristic dimension with unit of meter, $\frac{I^2}{W+r_{up}}$ is proposed in this project.

In addition, it is found that the use of $W + r_{up}$ as the characteristic dimension results in variation of Strouhal number of $0.30 \leq Sr_{W+r_{up}} \leq 0.43$. The use of W as the characteristic dimension has led to larger variation of Strouhal number in the range of $0.09 \leq Sr_W \leq 0.29$. The smallest variation in Strouhal number is observed when $\frac{I^2}{W+r_{up}}$ is used as the characteristic dimension, which is limited to $0.05 \leq Sr_{\frac{I^2}{W+r_{up}}} \leq 0.13$. It is therefore concluded that $\frac{I^2}{W+r_{up}}$ is the optimal choice of characteristic dimension. This finding is significant as it can allow us to avoid critical flow condition to minimize and prevent the whistling phenomenon more accurately and effectively

by using equation 4.1 and 4.2. It is also possible to design the pipe parameters if the flow condition cannot be manipulated in certain conditions.

Lastly, the simulation method proposed in this project is able to contribute effectively in the research of flow induced acoustics in corrugated pipe. This is because the simulation method is able to save cost, time and space compare to experimental method while not compromising the accuracy of the results obtained. In other words, large amount of information can be obtained by using simulation methods which are especially useful for the researchers in understanding the science and arts behind this topic of interest.

5.2 Recommendations

5.2.1 Multiple Cavities and 3D Simulation

One of the assumptions that was made in this project is the representation of entire flow condition with only single cavity. Although flow across a single cavity does give sufficient information on the acoustic pressure wave sources' characteristics in the corrugated pipes, further improvement can be made in the future by modelling multiple cavities in the simulation process. This method could possibly allow a more accurate observation of flow interaction between vortices although it is more computational expensive than the single cavity solution.

On the other hand, it is suggested that 3D simulations should be performed by using other simulation softwares such as Ansys Fluent. Even though the results obtained from 2D simulations are closely resembled to experimental results, further improvement can be made by using 3D simulations so that more accurate results can be obtained. In addition, more details of flow pattern of the fluid in the corrugated pipe can be investigated which could lead to a better understanding of the whistling phenomenon.

5.2.2 Experimental Method

Although some bench markings have been made to ensure the 2D simulation method is reliable, it is still advisable that if experimental method can be conducted so that every result obtained from the simulation can be compared to experimental method. The conduction of experiment can increase the confidence level of the results obtained. Besides, it can also lead to a better understanding of the actual flow situations in the corrugated pipe, which will be useful in solving the whistling issue. Table 5.1 is a list of all the equipment and material needed for the experiment.

Table 5.1: Equipment and Material Needed for Experiment

Equipment/Material	Qty
Pressure Vessel with Pressure Control Valve	2
Turbine Flow Meter	1
Flow Manipulating Valve	1
Measurement Section	2
Corrugated Pipe Segment	1
Microphones	4
Dynamic Signal Analyser	1
Computer	1

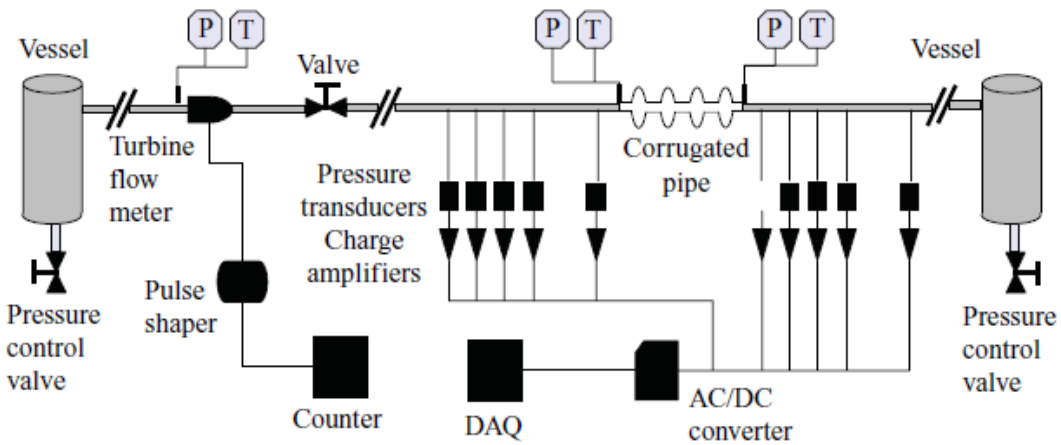

Figure 5.1: Experimental Setup

The experimental setup is shown in Figure 5.1 (Nakiboğlu et al., 2011) which is exactly the same as the experimental setup produced by Nakiboğlu et al. (2011). Basically, the setup consists of (from upstream to downstream) a pressure tank, a flow meter, a flow manipulating valve, a 1.6m long measurement tube, a corrugated pipe, another 1.6m long measurement tube and another pressure tank.

Nevertheless, instead of using 10 units of microphones, only 4 units of microphones is suggested in this project to save the cost. Besides, pulse shaper and counter are not required. The three sets of temperature and pressure sensor are also not required as suggested by (Nakiboğlu et al. (2011)) since the corrugated pipe segment is usually shorter than 10m.

On the other hand, the two straight measurement sections are used at upstream and downstream of the corrugated pipe respectively to facilitate the installation of the microphones. The microphones are connected to the four analogue channels of the dynamic signal analyser (as shown in Figure 5.2) which is then connected to the computer. The measurement software that is used in the computer is known as imc Devices 2.6.

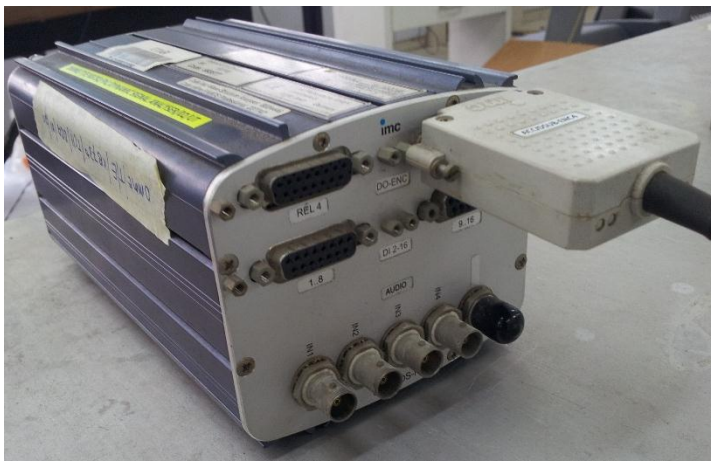

Figure 5.2: Dynamic Signal Analyser

The steps of using imc Devices 2.6 to obtain data such as sound level (dB), frequency and Strouhal number are very simple. After the dynamic signal analyser is connected, the device is configured to active status as shown in Figure 5.3. At this step, it is also important to define the sampling duration, sampling period and number of samples.

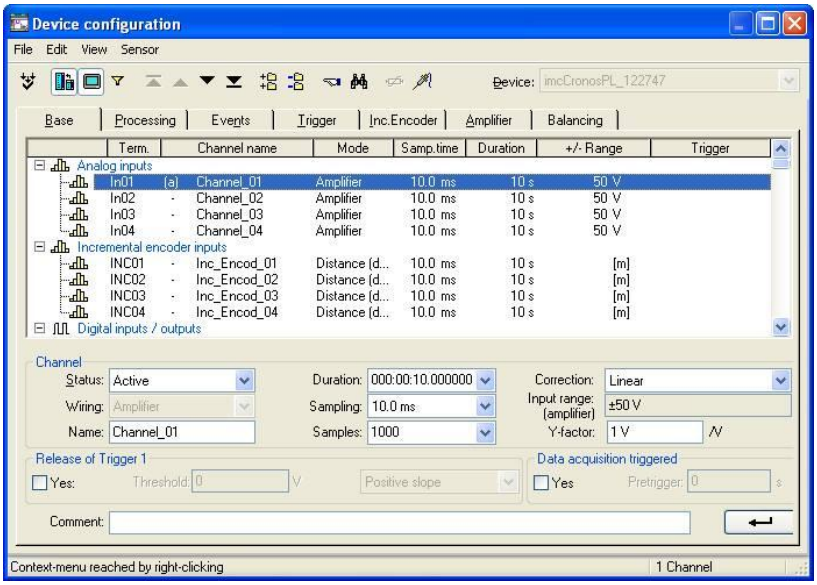

Figure 5.3: Device Configuration in imc Devices 2.6

After that, it would be necessary define the function used. For instance, with the pressure amplitude obtained from the microphone, it is possible to convert this pressure signal into dB which is a representation of sound level by using a ‘dB’ function as shown in Figure 5.4.

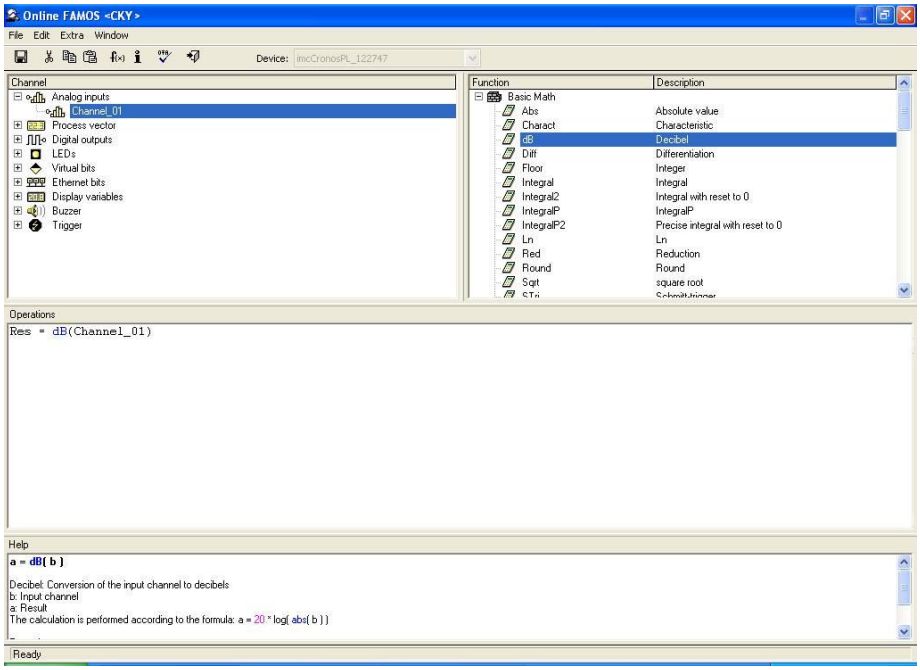

Figure 5.4: dB Function in imc Devices 2.6

Lastly, the information such as sound level, frequency and Strouhal number can be accurately captured and recorded after all the functions are defined correctly. These information can then be analysed and compared with the results obtained from the simulation method.

REFERENCES

Gao, Y., Zong, Z. & Sun, L. 2011. Numerical prediction of fatigue damage in steel catenary riser due to vortex-induced vibration. *Journal of Hydrodynamics, Ser. B,* 23**,** 154-163.

Martinez-Lera, P., Golliard, J. and Schram, C., 2010. Numerical study of flow-induced pulsations in pipe systems with closed branches. In: *16th AIAA/CEAS Aeroacoustics Conference*. Sweden, 8 June 2010. Reston: American Institute of Aeronautics and Astronautics.

Kristiansen, U. R. & Wiik, G. A. 2006. <Experiments on sound generation in corrugated pipes with flow.pdf>. *Acoustical Society of America,* 121**,** 1337–1344.

Nakiboğlu, G., Belfroid, S. P. C., Golliard, J. & Hirschberg, A. 2011. On the whistling of corrugated pipes: effect of pipe length and flow profile. *Journal of Fluid Mechanics,* 672**,** 78-108.

Nakiboğlu, G., Belfroid, S. P. C., Willems, J. F. H. & Hirschberg, A. 2010. Whistling behavior of periodic systems: Corrugated pipes and multiple side branch system. *International Journal of Mechanical Sciences,* 52**,** 1458-1470.

Nakiboğlu, G. & Hirschberg, A. 2012. Aeroacoustic power generated by multiple compact axisymmetric cavities: effect of hydrodynamic interference on the sound production. *Physics of Fluids,* Vol. 24**,** p067101.

Nakiboğlu, G., Manders, H. B. M. & Hirschberg, A. 2012. Aeroacoustic power generated by a compact axisymmetric cavity: prediction of self-sustained oscillation and influence of the depth. *Journal of Fluid Mechanics,* 703**,** 163-191.

Nakiboğlu, G. R., Oleksii; Hirschberg, A. 2012. Aeroacoustics of the swinging corrugated tube: Voice of the Dragon. *The Journal of the Acoustical Society of America,* vol. 131**,** p. 749.

Popescu, M., Johansen, S. T. & Shyy, W. 2011. Flow-Induced Acoustics in Corrugated Pipes. *Communications in Computational Physics*.

Tonon, D., Landry, B. J. T., Belfroid, S. P. C., Willems, J. F. H., Hofmans, G. C. J. & Hirschberg, A. 2010. Whistling of a pipe system with multiple side branches:

Comparison with corrugated pipes. *Journal of Sound and Vibration,* 329**,** 1007-1024.